IHEP, Seminar, Nov. 25, 2024

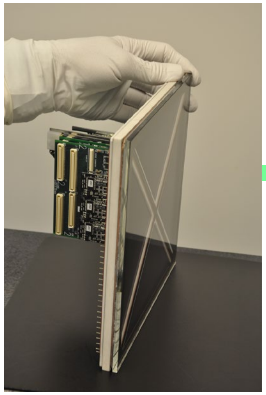
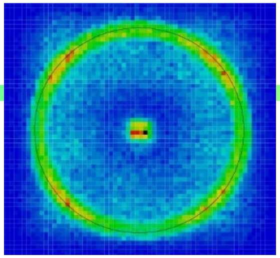
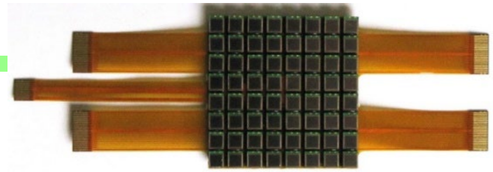
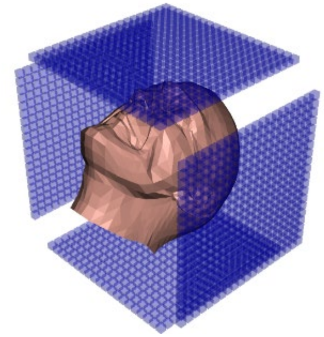

Instrumentation for advances in PET medical imaging

Peter Križan

University of Ljubljana and J. Stefan Institute

Interplay of detector R&D for particle/nuclear physics and medical imaging

Traditionally excellent collaboration of the two research areas.

Novel detection techniques required in particle physics →with modifications often applications are possible in medical physics

… and sometimes also vice versa…

One of the recent examples: SiPMs as scintillation light sensors for

- Electromagnetic calorimeters, RICH counters
- Positron Emission Tomography (PET) scanners

Our original expertise: Cherenkov detectors, single-photon sensors and associated electronics

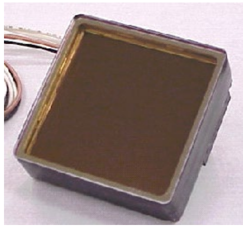

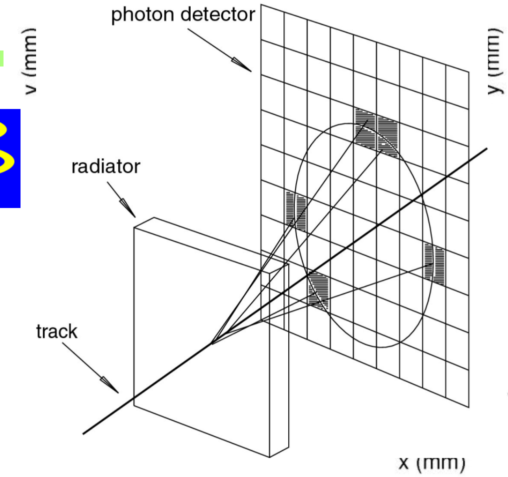

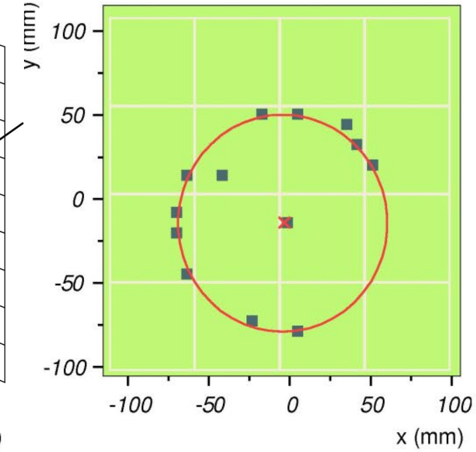

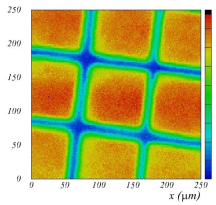

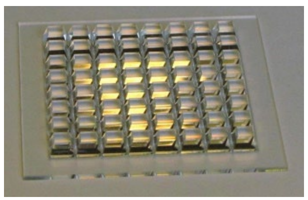

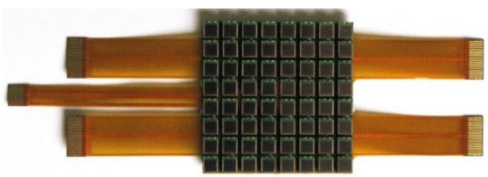

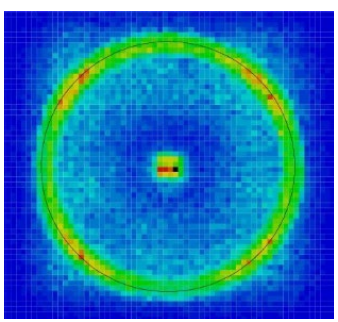

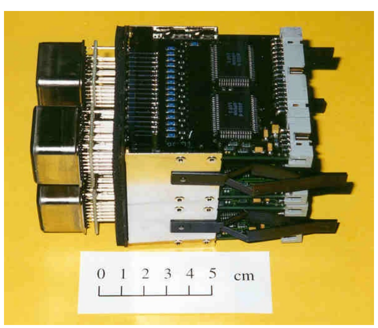

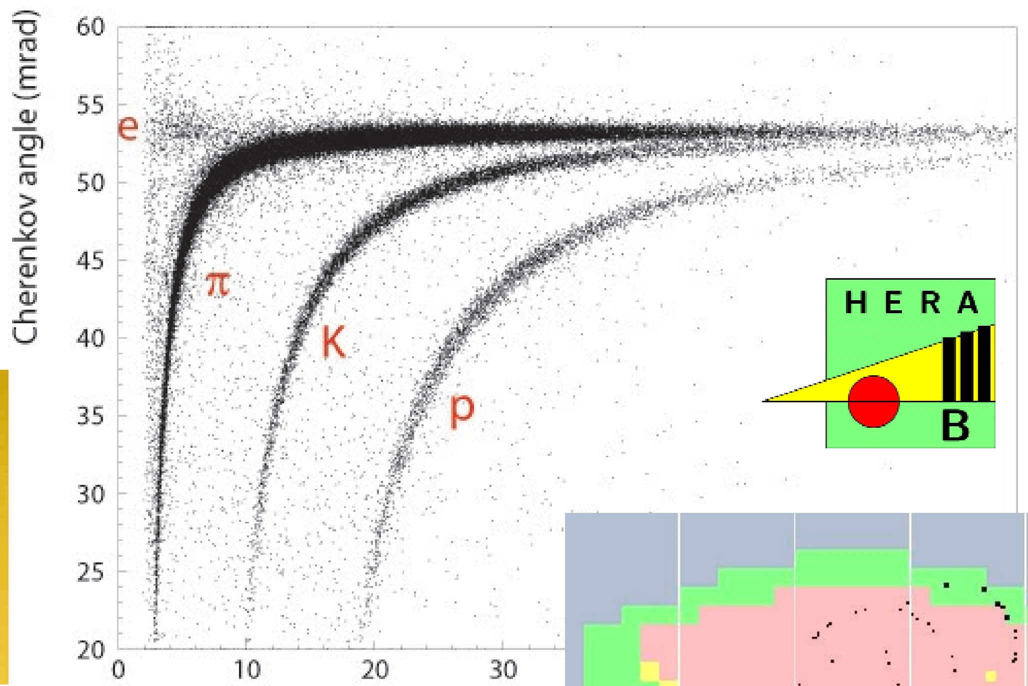

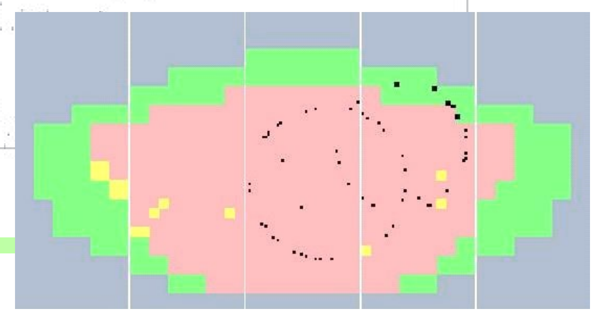

Belle II Detector

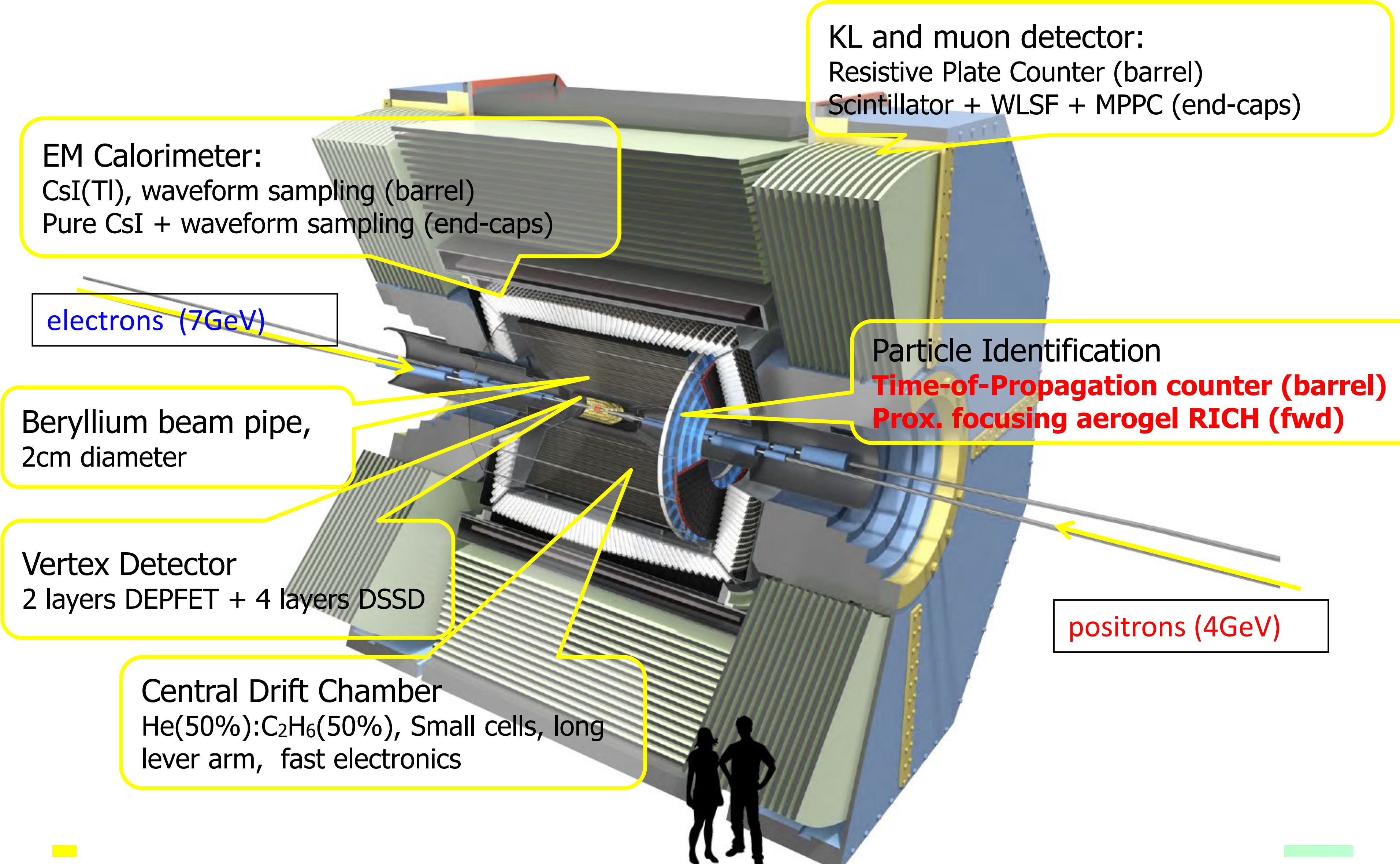

bljana

Contents

PET – Positron Emission Tomography

Current topics in PET

Flexible limited angle PET scanner

Cherenkov radiation-based PET scanner

Conclusions and summary

PET: positron emission tomography

In the blood of the patient, a substance is administered that contains a radioactive isotope – a beta+ emitter (e.g., fluorodeoxyglucose, FDG, with ^{18}F).

Positrons from the ^{18}F decay annihilate with electrons in the tissue, emitting a pair of collinear gammas.

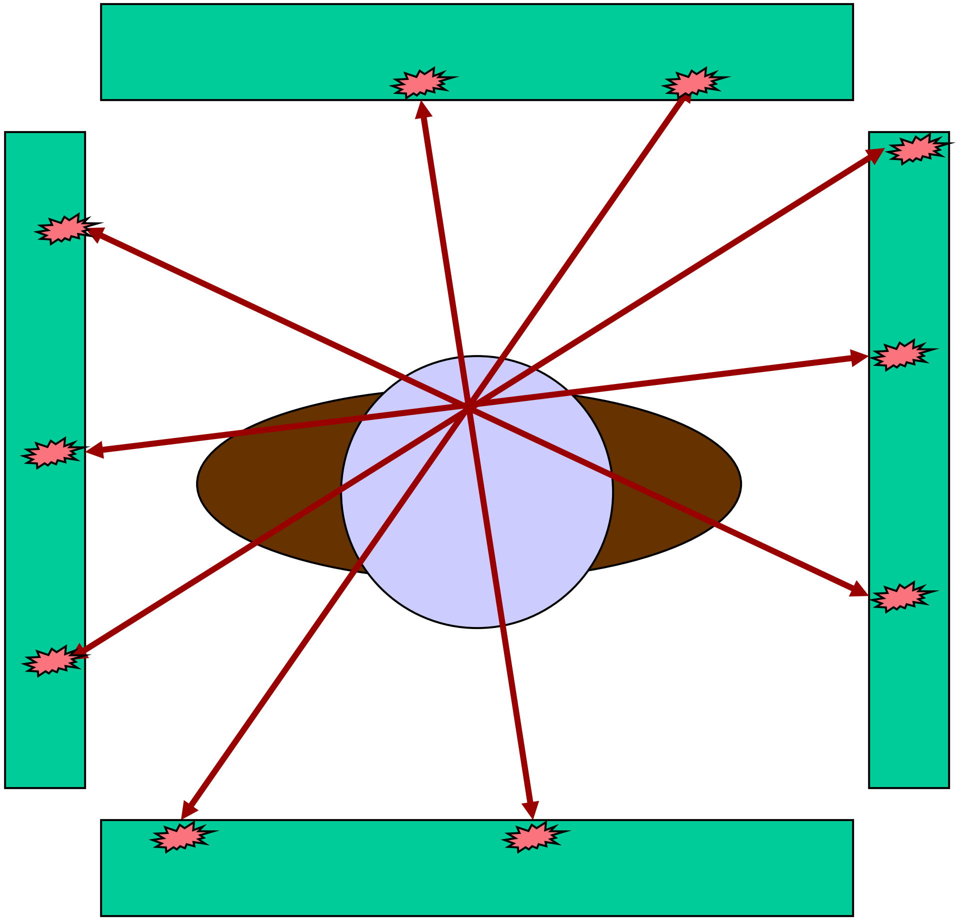

PET: collection and handling of data

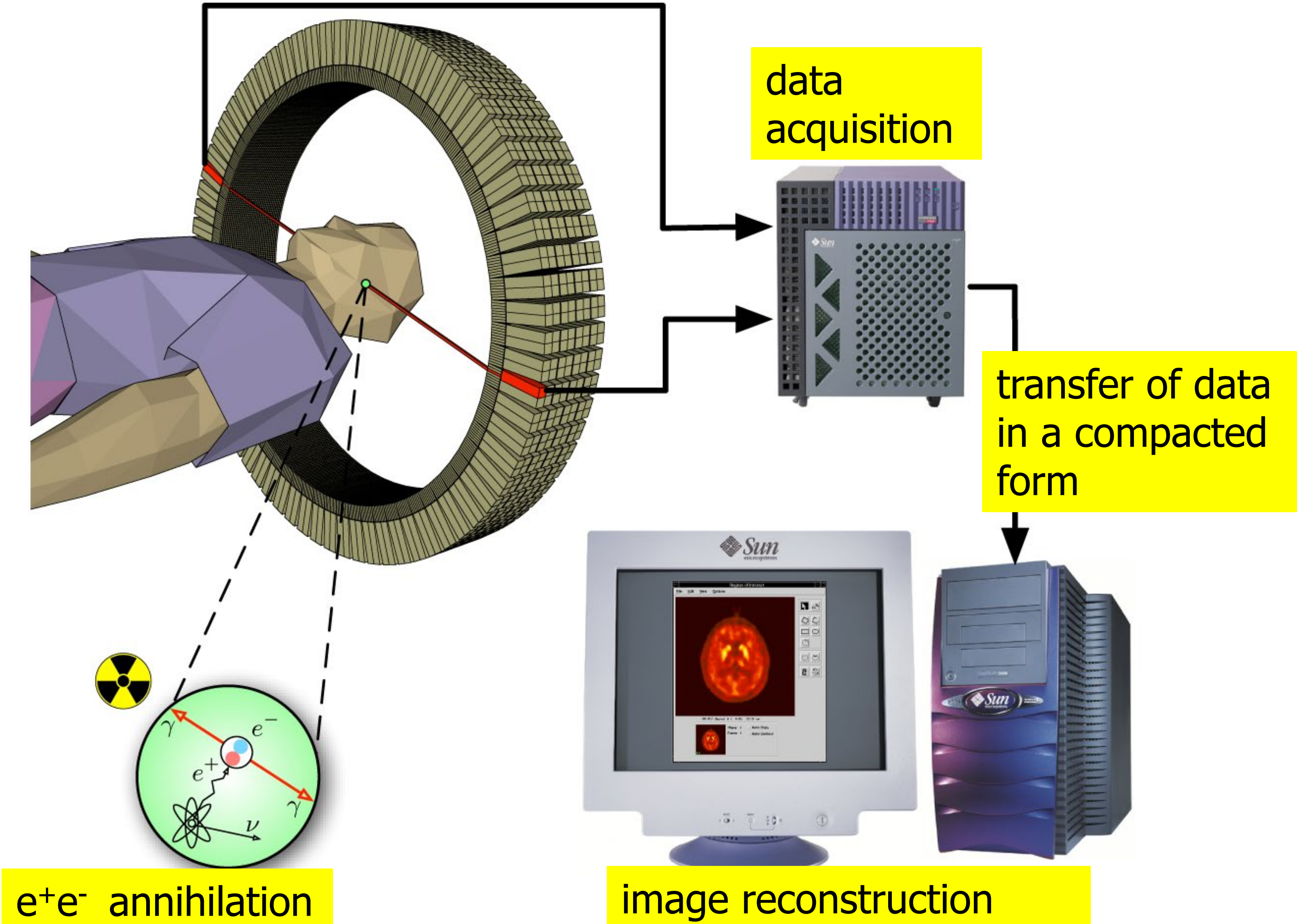

PET: image reconstruction

Image reconstruction: from the position and direction of the lines determine the distribution of the radioactive fluorine in the body.

The places in the body with a higher substance concentration will show a higher activity.

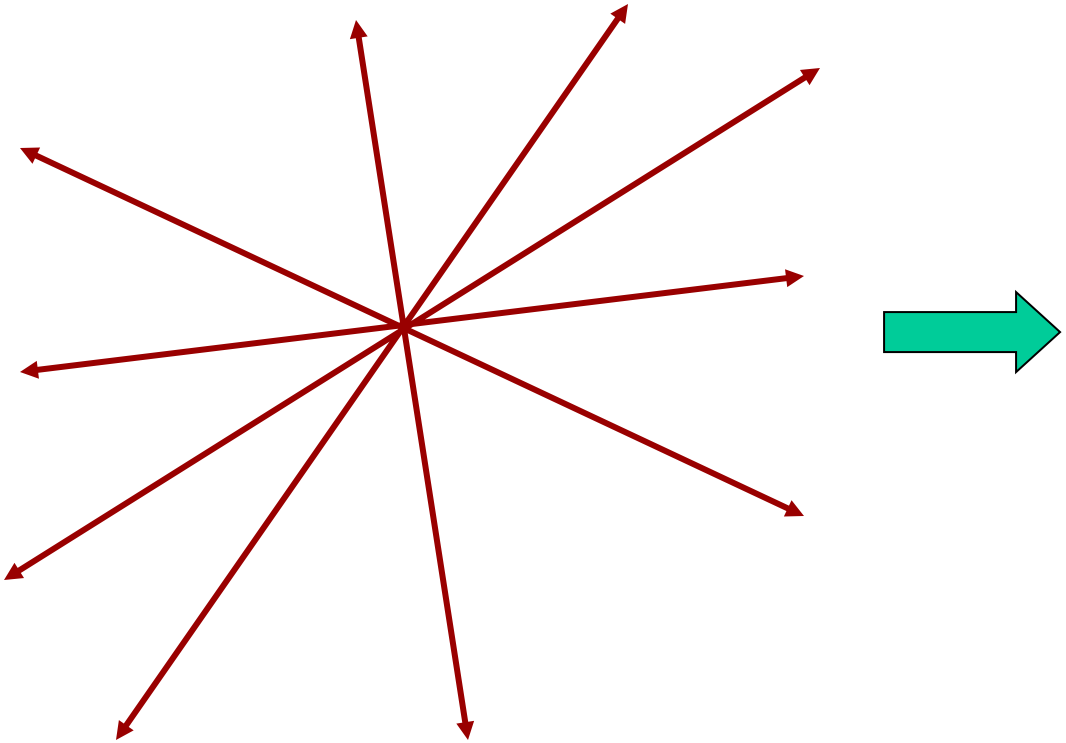

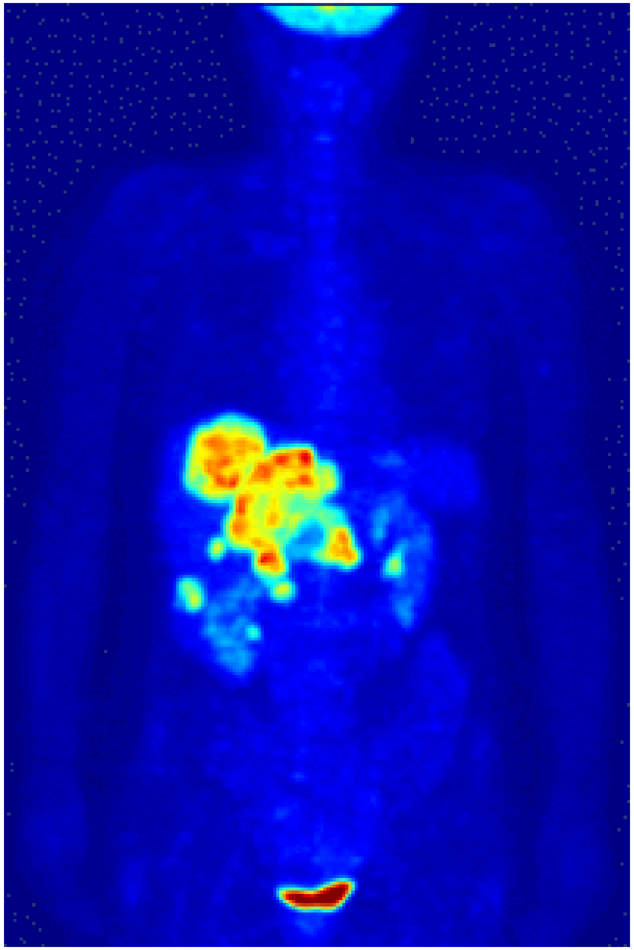

PET with a time-of-flight information

The emission point of the γ pair can be anywhere on the line between the two detector elements that have been hit.

Detectors can in principle also measure the time of arrival of each of the γ rays

→ an additional constraint on the point of origin of the two γ rays along the line connecting the two detector hits

→ time-of-flight (TOF) PET

Good resolution in time-of-flight → limits the number of hit pixels along the line connecting the two detector hits

In the reconstruction step, each line contributes to fewer pixels

→ less noise in the reconstructed image

No TOF

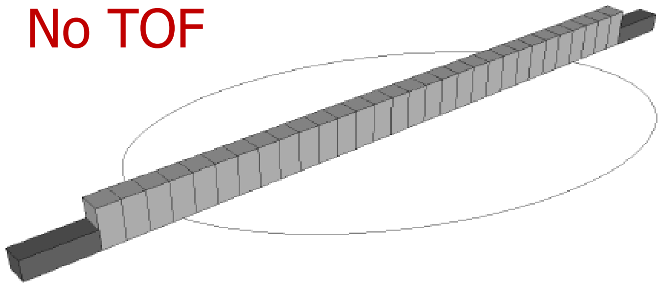

TOF

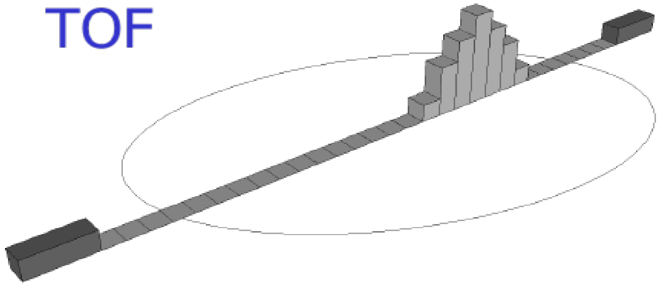

TOF-PET: positron tomography with the time-of-arrival measurement

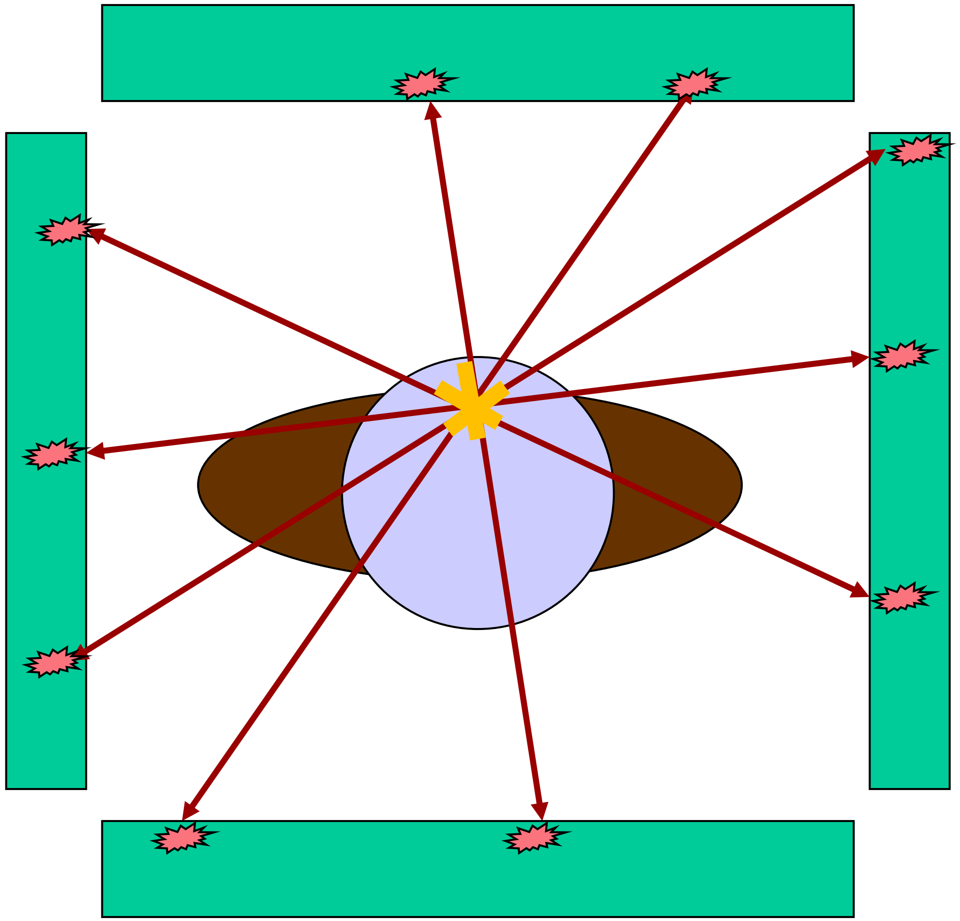

Good resolution in time-of-flight → limits the number of hit pixels along the line connecting the two detector hits

In the reconstruction step, each line contributes to fewer pixels

→ less noise in the reconstructed image

TOF-PET: time resolution

What kind of time resolution is needed?

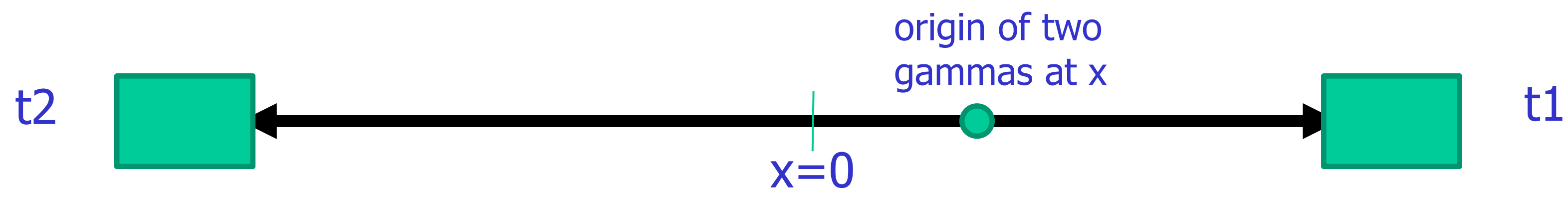

$t1 = (L/2 - x)/c$ source at x, distance between detectors = L

$t2 = (L/2 + x)/c$

$t1 - t2 = 2x/c \rightarrow x = (t1 - t2)\, c/2 \rightarrow \Delta x = \Delta(t1\text{-}t2)\, c/2$

resolution in TOF $\Delta(t1\text{-}t2) = 300$ ps $\rightarrow \Delta x = 4.5$ cm

$\Delta(t1\text{-}t2) = 66$ ps $\rightarrow \Delta x = 1$ cm

$\Delta(t1\text{-}t2)$ – CTR, coincidence timing resolution (FWHM)

Effective sensitivity $$S_{\mathrm{eff},D} \propto \eta_{\mathrm{det}}^2\, \eta_{\mathrm{geom}} \frac{D}{\Delta t}$$

- η_{det} - detection efficiency of the detector
- η_{geom} - the geometrical efficiency (angular coverage)
- D - diameter of the object imaged
- Δt - coincidence timing resolution - CTR

Optimize detector CTR (Δt) to maximize the sensitivity

Motivation for Fast TOF PET

- Paradigm shift in medicine:
  - From the treatment of an obvious disease
  - To early diagnosis / prevention
- This leads to more stringent requirements on PET diagnostics
  - Sensitivity (=positive→positive)
  - Specificity (=negative→negative)
- Targeted Radionuclide Therapy (TRT) & Theranostics*
  - introduced an urgent need for more widespread and accurate PET

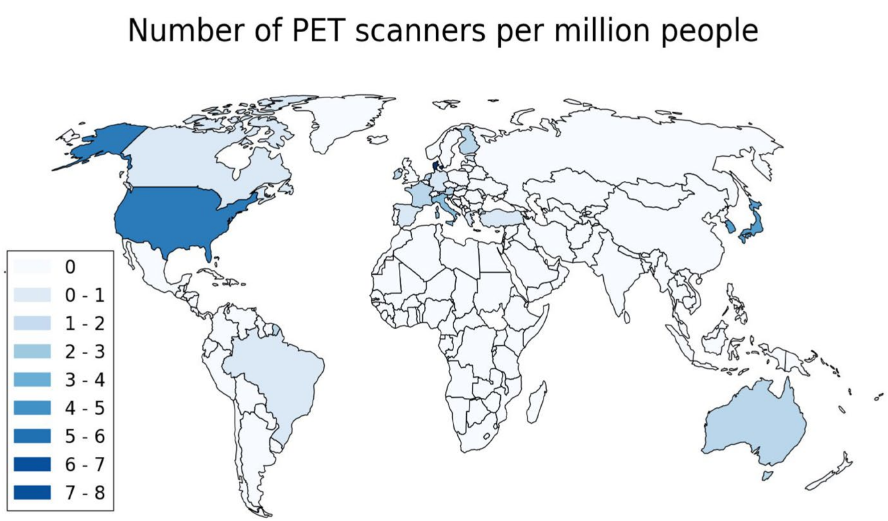

*Theranostics is a two-pronged approach to diagnosing and treating cancers through the use of radiotracers. Radiotracers are compounds made of chemicals that selectively bind to a specific target in the body, and of a radiative component. In the diagnostic phase, the radioactive part is a beta emitter, while in the treatment phase it is a strong radiation source to damage the cancer cells.

Current situation

- Standard clinical scanners are sub-optimal:
  - Cost of equipment, limited access, performance.
- Novel long axial PET scanners offer a very attractive solution in terms of
  - increased sensitivity and
  - enabling fast pharmacokinetics/pharmacodynamics.
- They pose significant challenges both
  - Financially
  - Logistically

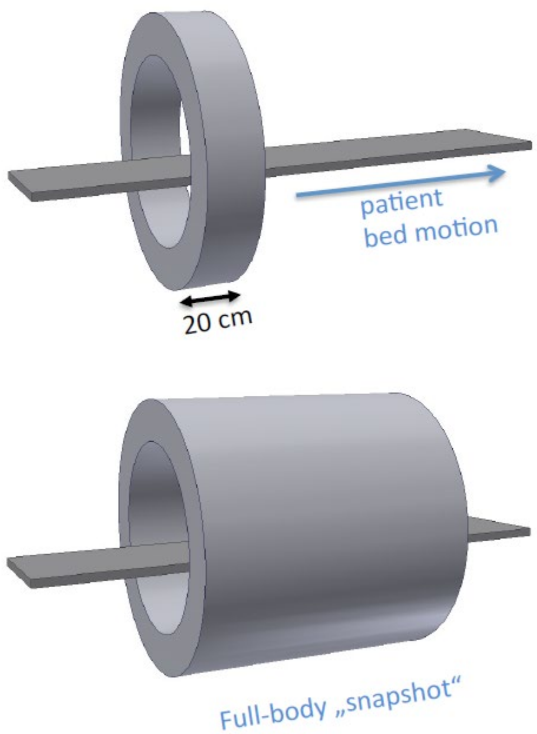

State-of-the-art in TOF PET

Essential parameter: CTR – coincidence timing resolution

https://www.siemens-healthineers.com/molecular-imaging/pet-ct/biograph-vision

- Clinical scanner:
  - Siemens Biograph Vision PET/CT → **214 ps**

- Laboratory measurement:
  - Gundacker *et al, Phys. Med. Biol.* 65 (2020) 025001 (20pp)

2 x 2 x 3 mm LSO → **58 ps***

2 x 2 x 20 mm LSO → 98 ps*

*measured with single crystals with high-power readout electronics that cannot be scaled to large devices

Gamma detectors for PET

Scintillating crystal:

- converts gamma energy into optical photons

Photodetector

- converts optical photons into electrical pulses

Time resolution in TOF PET limited by

- scintillation light emission ‘10 ps challenge’
  - rise and decay time
- **optical photon travel time spread in the crystal**
- **photodetector response**
- **readout electronics**

Limitations on timing due to optical travel time

Inherent limitation for any crystal-based annihilation gamma detector:

- optical photons, produced in the crystal, need to reach the photodetector
- inside the crystal, optical photons propagate at a lower speed (c/n) than gamma rays (c)
- refractive index, crystal dimensions → intrinsic travel time spread due to different gamma interaction depths
- for a 15 mm long crystal this contribution is > 40 ps FWHM:

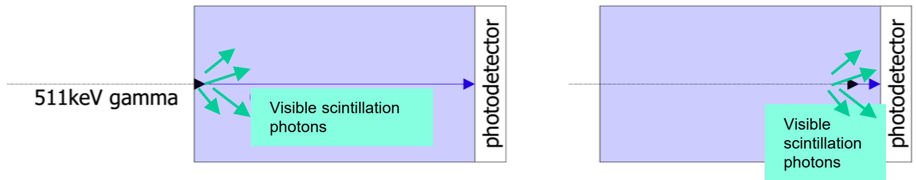

d = 15 mm, n = 1.8: $t = d \cdot n/c_0 = 90$ ps $t = d/c_0 = 50$ ps $\rightarrow \Delta t = 40$ ps

- Can in principle be corrected for by:
  - measuring the depth of interaction (DOI)
  - building the detector with shorter crystals → multi-layer configuration

Can we simplify the TOF PET scanner

– and make it cheaper and flexible?

Next generation scalable time-of-flight PET

Superb time resolution enables simplifications in the scanner design

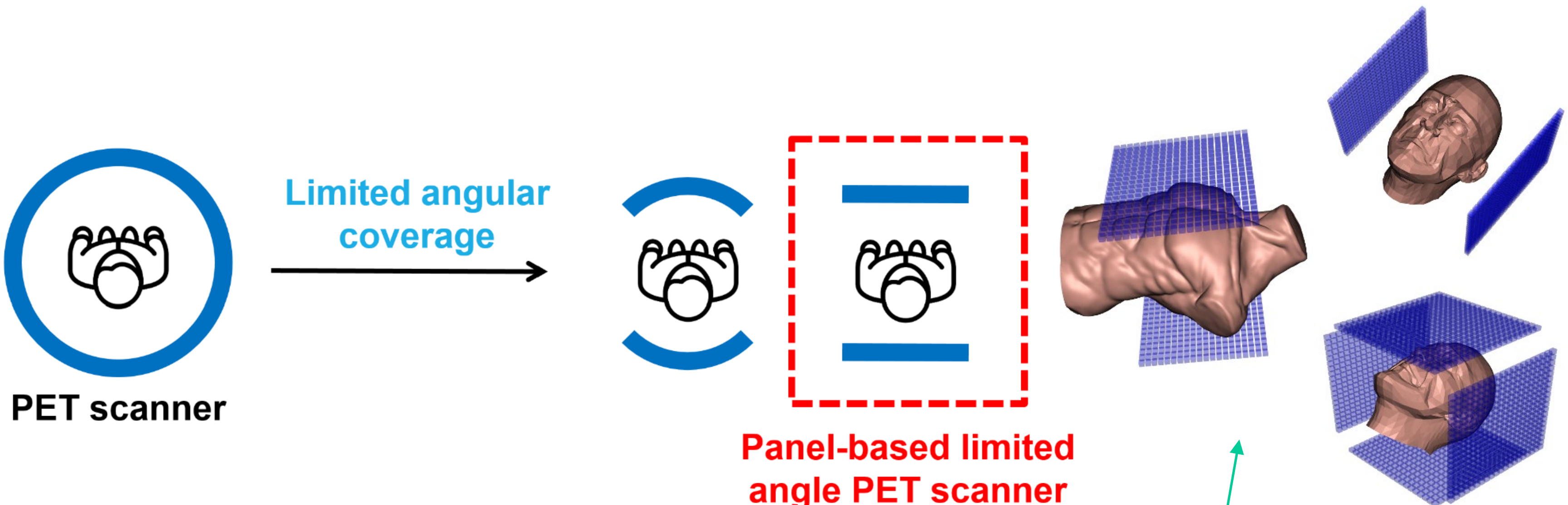

Limited angle PET scanners will generally produce distorted images with artefacts - unless they have good **time-of-flight** information

S. Surti, J. S. Karp, Phys. Med. Biol. 53 (2008) 2911

G. Razdevšek *et al.*, IEEE TRPMS 6 (2022) 721

Potential benefits of a panel-based PET system

Mobility

– Portable or bedside PET imaging

Flexibility

– Adjustable FOV and sensitivity

Modularity

– Combining multiple panels → multi-organ/total-body PET scanner

Accessibility

– Reduced manufacturing cost and complexity

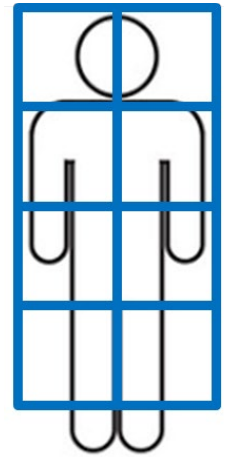

Simulation of a limited angle system

Geant4/GATE → Monte Carlo simulations of digital phantoms and different scanner designs

CASToR → image reconstruction with Maximum Likelihood Expectation Maximization (**MLEM**) algorithm

- Investigate the benefits of coincidence time resolution
- Study the performance **two-panel** and **four-panel** designs

Enabling Open Geometry systems

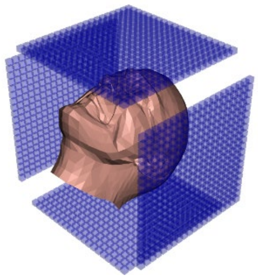

Two pairs of 30x30 cm^2
LYSO panels with 50ps CRT

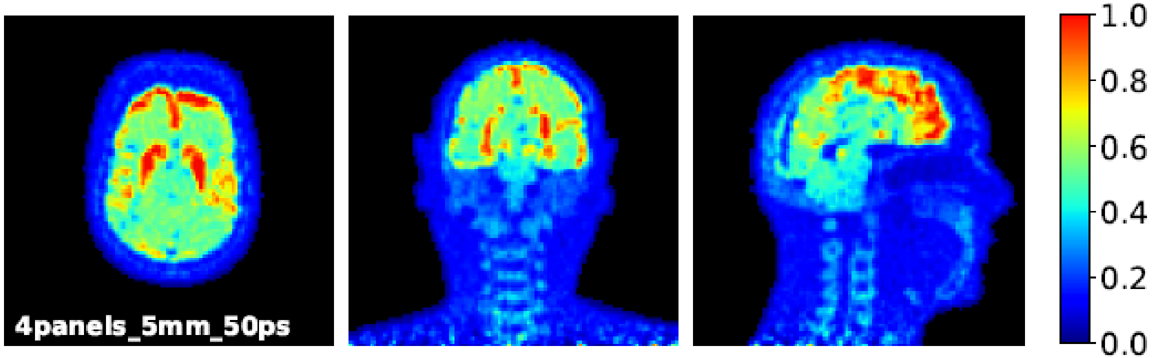

Similar performance as

Siemens Biograph Vision

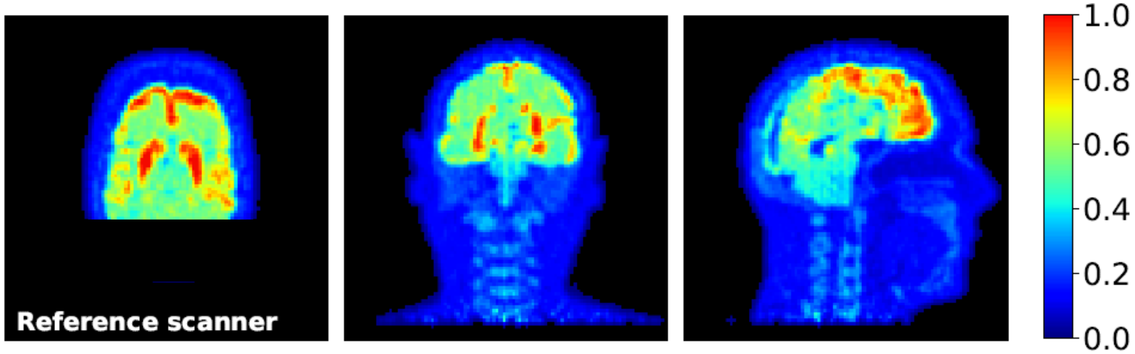

G. Razdevšek *et al.*, "Multi-panel limited angle PET system with 50 ps FWHM coincidence time resolution: a simulation study," IEEE TRPMS 6 (2022) 721, doi: 10.1109/TRPMS.2021.3115704.

Simulation study of planar configurations

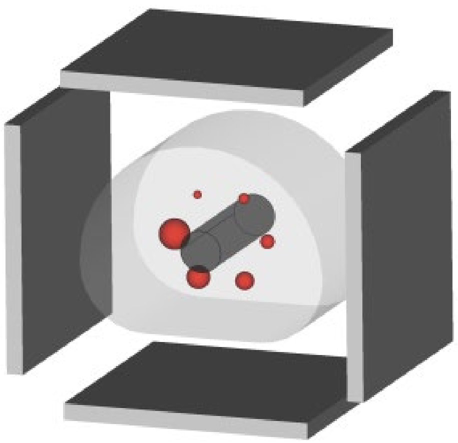

Simulated arrangement of 30x30 cm^2 flat panel detectors

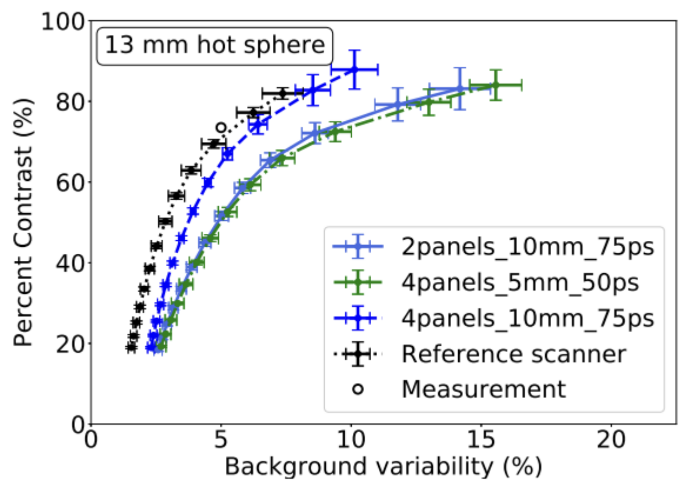

Percent contrast versus background variability (~noise level in the image)

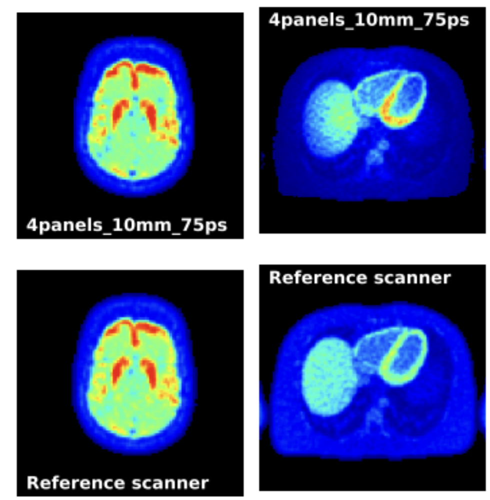

Reconstructed images of a torso and head for the flat panel detectors and the reference scanner Siemens BV

G. Razdevšek *et al.*, IEEE TRPMS 6 (2022) 721, doi: 10.1109/TRPMS.2021.3115704.

Design optimisation of a flat-panel, limited-angle TOF-PET scanner: simulation

Reconstructed NEMA phantom for various detector parameters.

Scanner: 3mm x 3mm x 10mm,
CTR=75ps

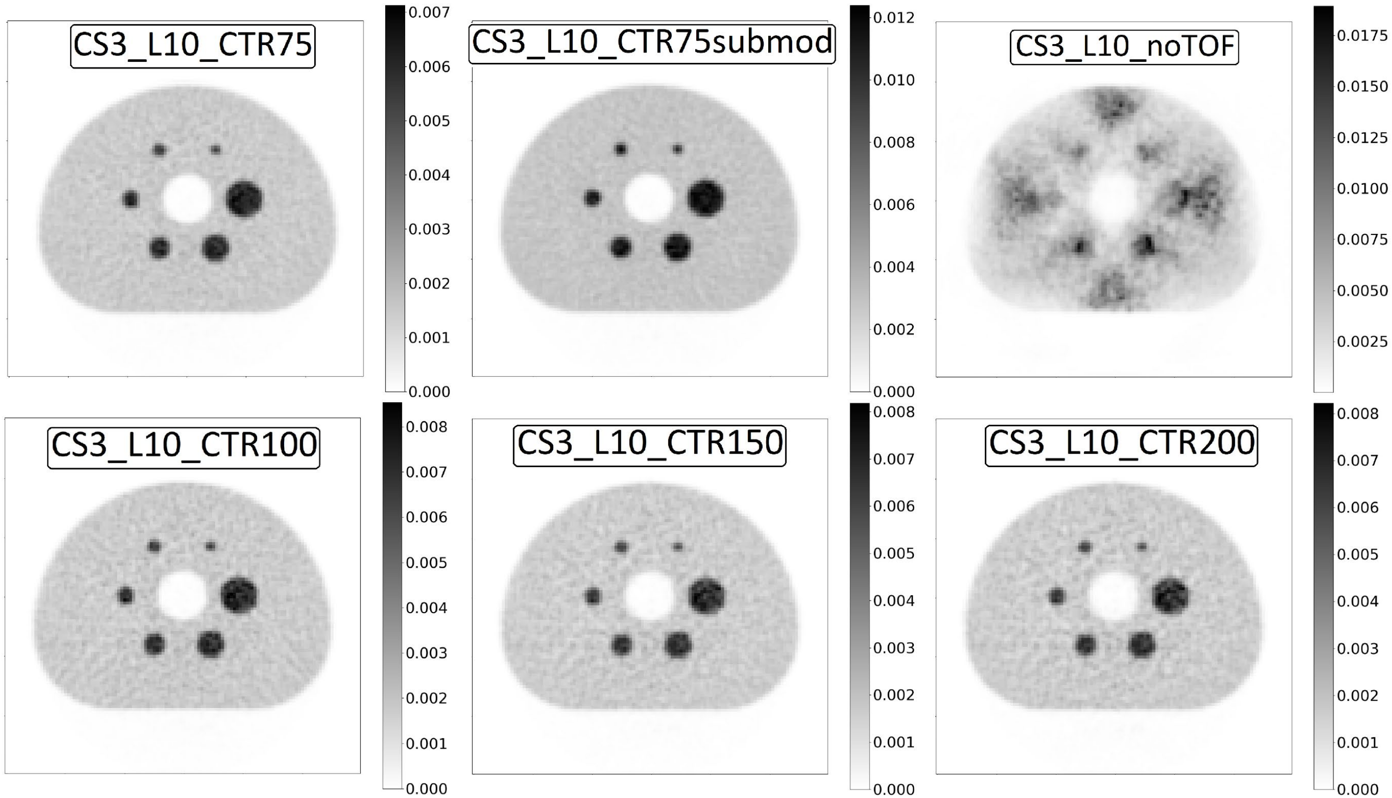

A 5 mm filter is applied to all of the images.

M. Orehar et al., Design Optimisation of a Flat-Panel, Limited-Angle TOF-PET Scanner: A Simulation Study. Diagnostics 14 (2024) 1976, doi: 10.3390/diagnostics14171976.

Design optimisation of a flat-panel, limited-angle TOF-PET scanner: simulation

Image quality plots for the 13 mm sphere for different scanner parameters.

Percent contrast vs background variability (~noise)

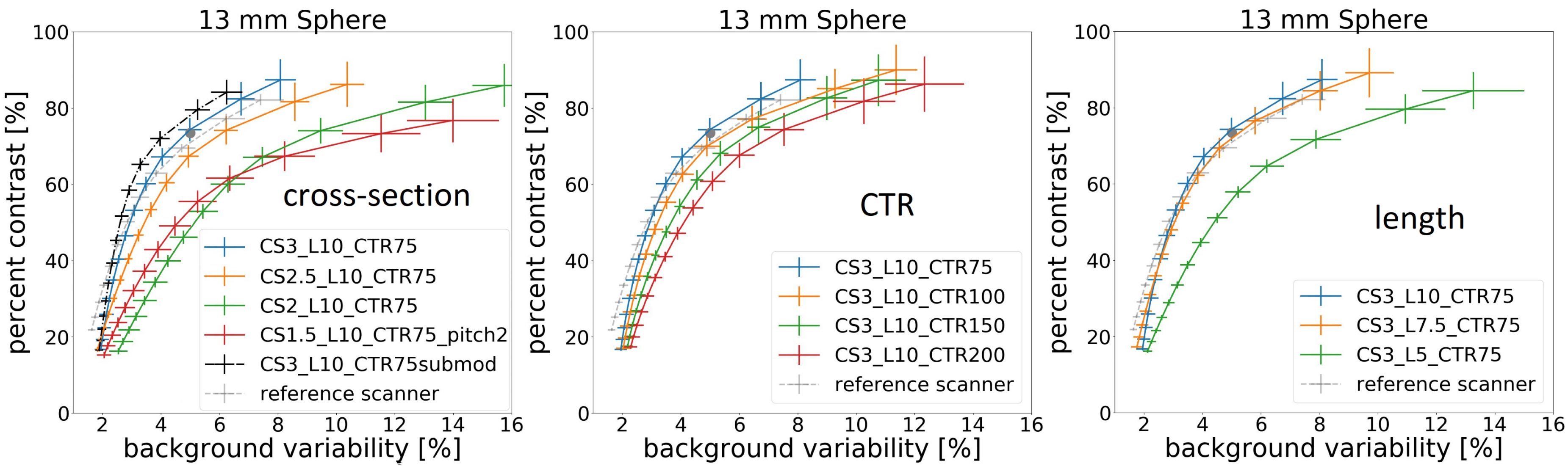

different crystal cross-sections and pitches

Impact of CTR

Impact of crystal length.

Grey circle: experimental measurement value for the reference scanner.

M. Orehar et al., Diagnostics 14 (2024) 1976

Design optimisation of a flat-panel, limited-angle TOF-PET scanner: simulation

Images of the brain phantom in the transverse plane

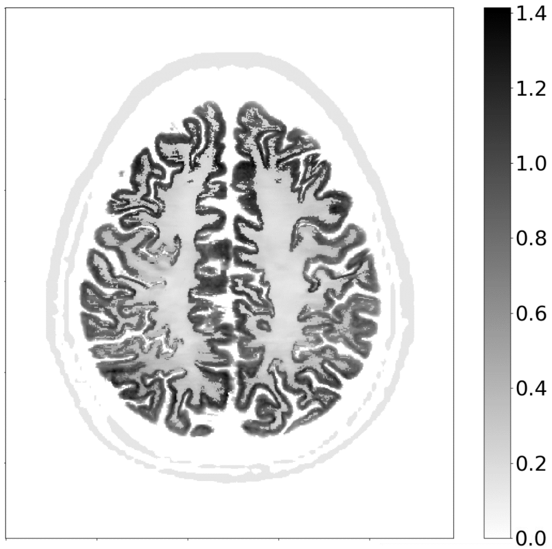

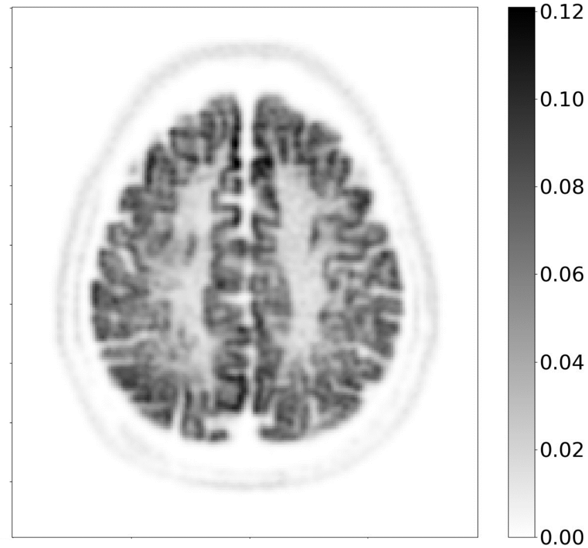

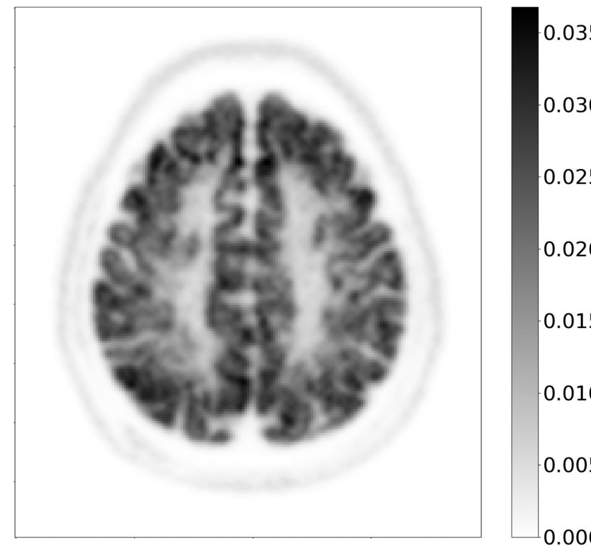

activity phantom

image reconstructed with the 3mm x 3mm x 10mm, CTR 75ps scanner

image reconstructed with the reference scanner.

M. Orehar et al., Diagnostics 14 (2024) 1976

From Limited angle to Total-body

Increased sensitivity by larger panels

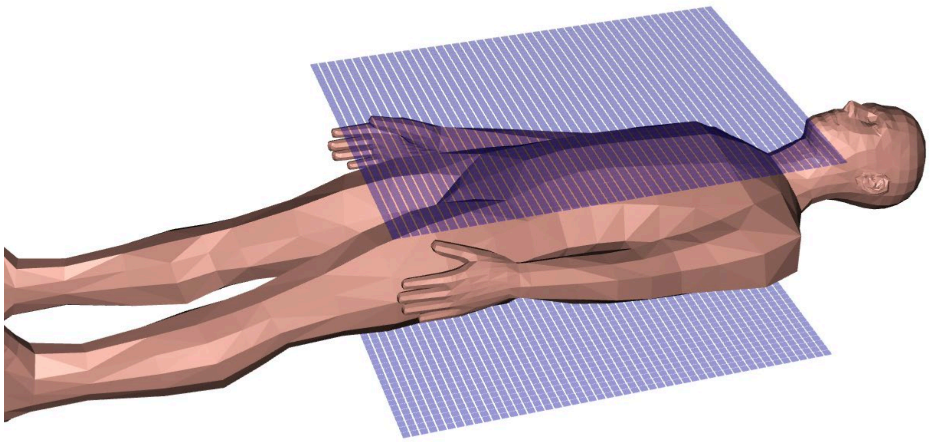

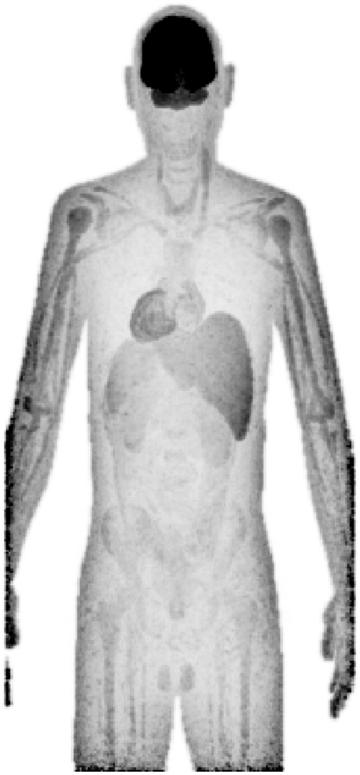

Capability of the planar TOF PET imager:
Image of a reconstructed 3 mm slice of an digital phantom acquired by two 120 x 60 cm^2 panel detectors (above and below the patient) assuming 100 ps TOF resolution and 10 mm LYSO scintillator thickness.

Next-generation scalable time-of-flight PET

Address PET system challenges of a limited angular coverage using fast CTR

Joint effort: JSI, FBK, ICCUB, I3M, Oncovision, TU Munich and Yale

- Front-end electronics: develop a low-noise, high-dynamic-range ASIC with a time resolution of 20 ps & on-chip TDC
- Improve SiPM sensor
- Explore 2.5 D integration with the photo-sensor to achieve sub-100 ps CTR

Aim: Improve (SNR) without increasing cost associated with axial coverage by resorting to very sparse angular coverage of the patient and long axial field coverage

Managed to get a 3 MEUR EIC EU grant for 5 years to further develop the method and construct a prototype.

https://petvision.org

PET VISION

Fast CTR PET module

How to achieve such a good CTR?

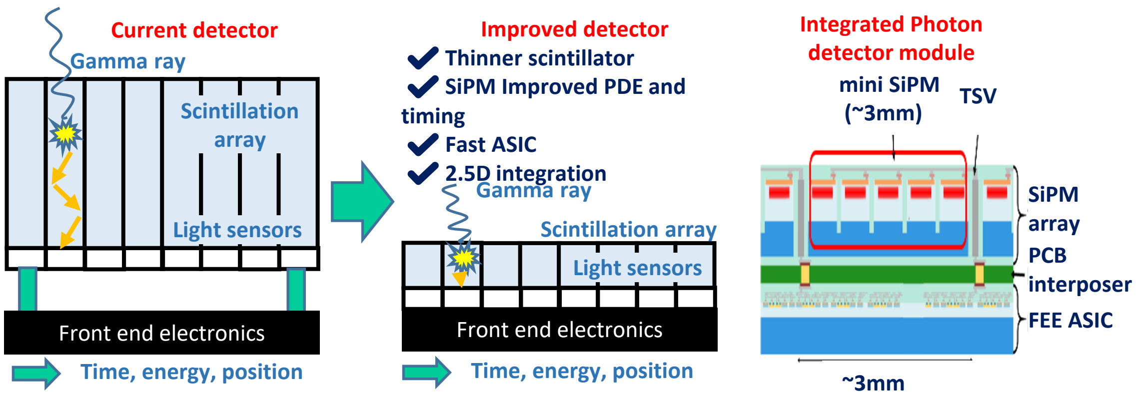

FastIC readout chip

FASTIC: ASIC for fast single photon sensors

- **Collaboration of ICCUB (Univ. Barcelona) and CERN**
- **8 Inputs:** 8 Single Ended (POS/NEG), 4 differential and summation (POS/NEG) in 2 clusters of 4 channels.
- **3 Output modes:** (1) SLVS; (2) CMOS; and (3) Analog.
- Active analog summation of up to 4 SE channels to improve time resolution

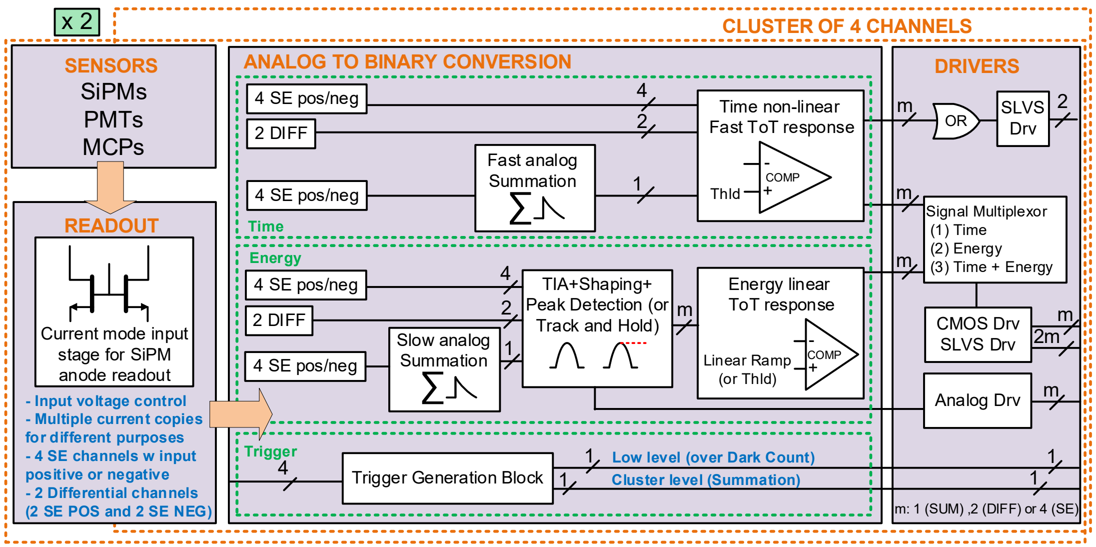

- High dynamic range with linear energy response
- Adapted to different detectors: LYSO/LSO, BGO, Cherenkov, Monolithic, etc

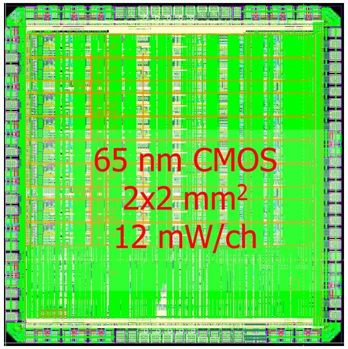

First results with FastIC

- **Sensor:** FBK-NUVHDLFv2b 3x3 mm², 40 pixel pitch.
- **Crystal:** LSO:Ce Ca 0.2% of 2x2x3 mm³.

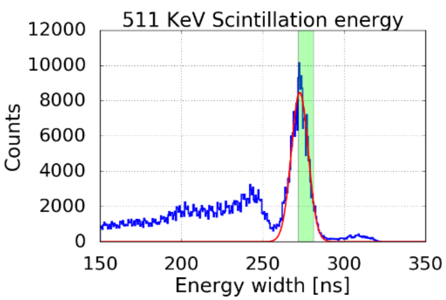

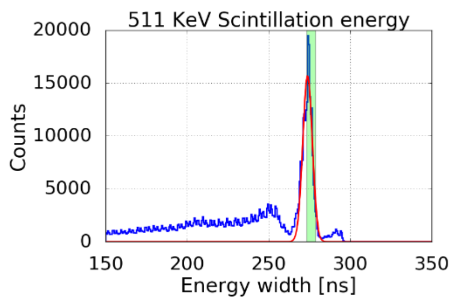

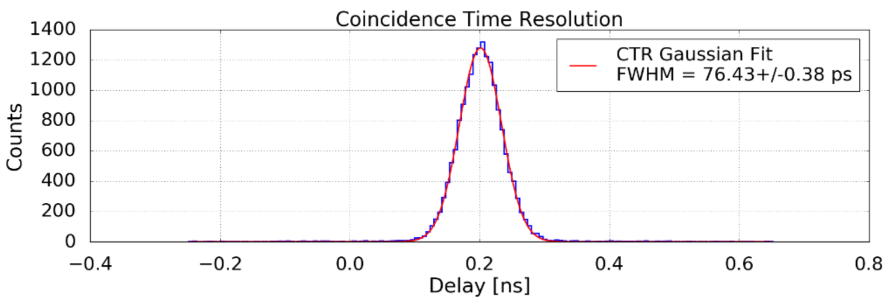

FWHM = 76.43 ps

Pairs of annihilation gammas

Single photons

- **SPTR with** FBK-NUVHDLFv2b 3x3

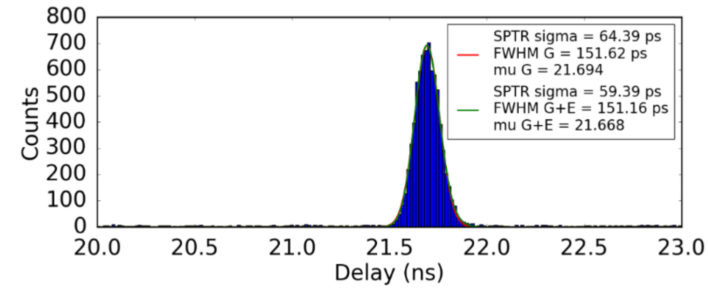

- CTR versus crystal length for LYSO and LSO

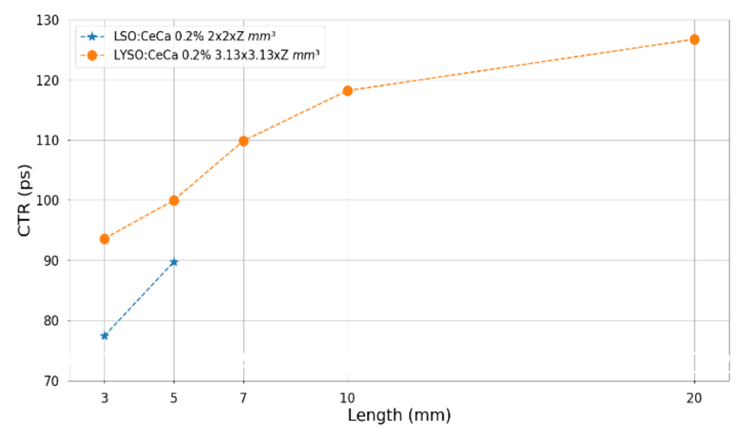

D. Gascon, talk at Instrumentation for the future of particle, nuclear and astroparticle physics and medical applications in Spain, March 2023

Next generation ASICs

- ICCUB and CERN are working on FastIC+: integration of 25 ps bin TDC integration on FastIC

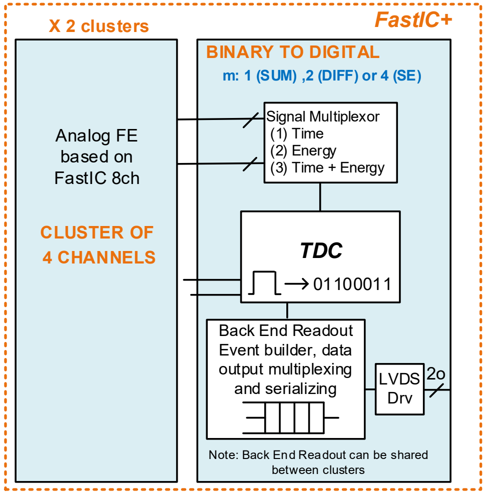

- On the longer term plan for a 32 ch. ASIC (FastIC32)
  - Pixelated structure: 2.5D (BGA, flip-chip, etc) or 3D integrated

FastIC 32

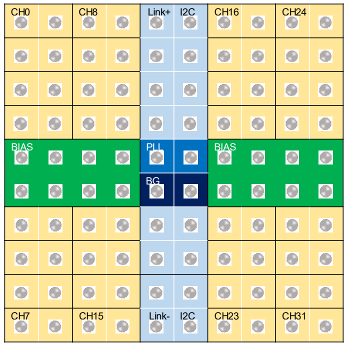

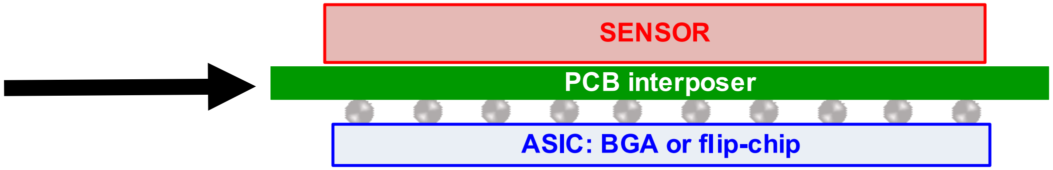

D. Gascon, talk at Instrumentation for the future of particle, nuclear and astroparticle physics and medical applications in Spain, March 2023

FBK SiPM sensor

2.5D integrated SiPM tile for improved timing

In the short and medium term - medium density interconnection

- excellent timing on large photosensitive areas w/o increasing complexity + cost too much.
- SiPMs with TSVs down to 1 mm pitch are connected to the readout ASIC on the opposite side of a passive interposer, in a 2.5D integration scheme.

Integrated Photon Detection Module

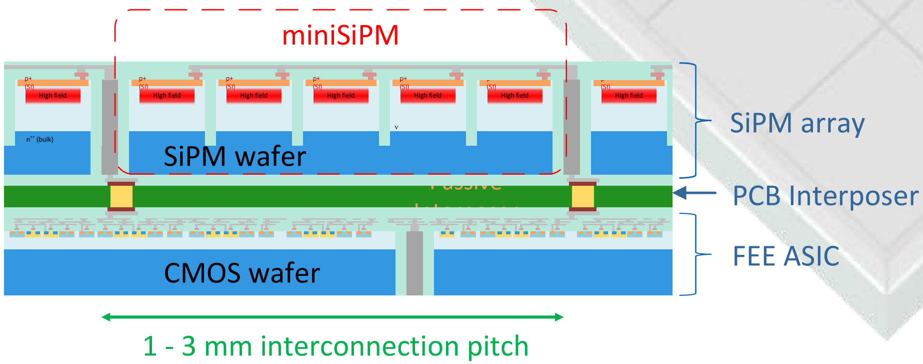

Hybrid SiPM module being developed for ultimate timing performance in TOF-PET

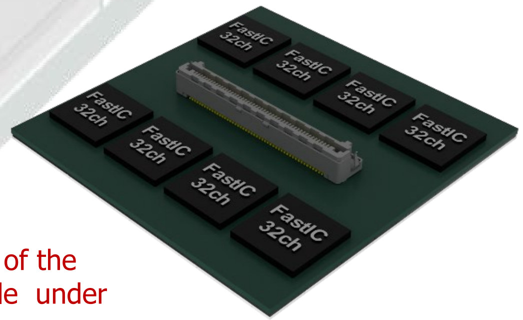

Conceptual drawing of the photon detector module under development

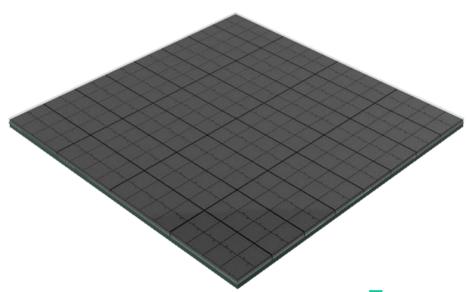

Limited angle PET scanner, conclusions

- Good coincidence time resolution can:
  - compensate for lower detection efficiency or smaller angular coverage
  - enable us to obtain good image quality with a simple limited angle PET system without distortions or artifacts

- We plan to enable open geometry designs and enable a wider spread of PET imaging by reducing different contributions to CTR :
  - Optimize scintillator thickness
  - Improve SiPM – TSV
  - Fast ASIC
  - 2.5D integration
  - If new – faster scintillators emerge, we should be able to make use of them

Use of Cherenkov light in TOF-PET

Use of Cherenkov radiation for TOF-PET

- lead fluoride (PbF_2) as Cherenkov radiator material

Previous work

Limitations of Cherenkov TOF-PET

- single photon detection - **limited scatter suppression**

Image quality with Cherenkov TOF-PET

-whole-body scanner simulations

-crystal readout configurations

-results

R. Dolenec[a,b], D. Consuegra Rodríguez[a], P. Križan[a,b], M. Orehar[b],
R. Pestotnik[a], G. Razdevšek[b], A. Seljak[a] and S. Korpar[a,c]

[a] **J. Stefan Institute**, Ljubljana, Slovenia
[b] Faculty of Mathematics and Physics, **University of Ljubljana**, Ljubljana, Slovenia
[c] Faculty of Chemistry and Chemical Engineering, **University of Maribor**, Slovenia

https://photodetectors.ijs.si/

Imaging Cherenkov detectors

Measure the Cherenkov angle (RICH counter)

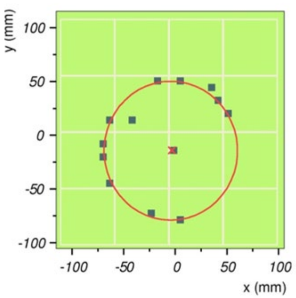

ARICH@Belle II

RICH@HERA-B

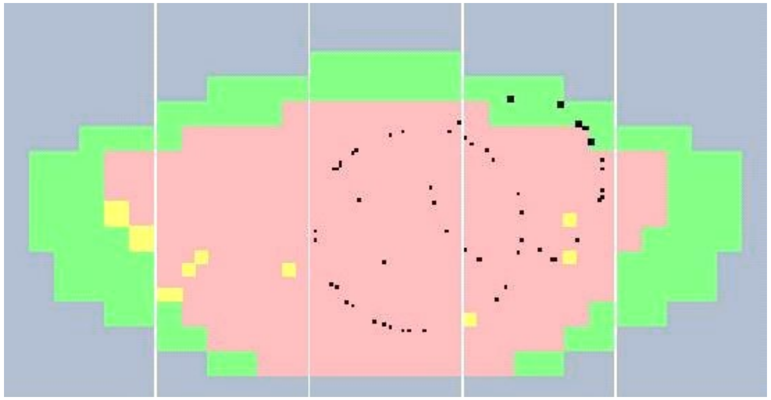

… or a pattern in the coordinate-vs-time space (TOP@Belle II)

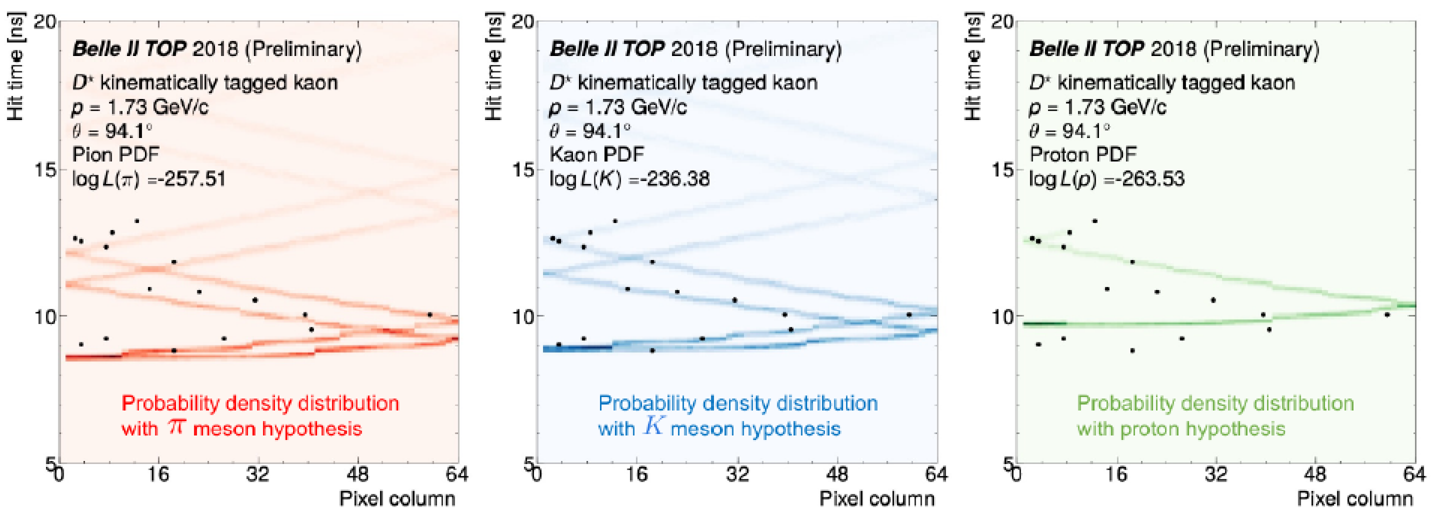

Use of Cherenkov Light in TOF-PET

γ detectors in traditional PET: scintillator crystal + photodetector

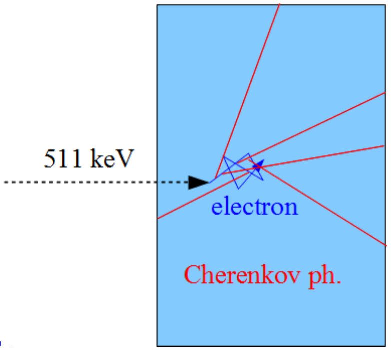

Charged particles (e^- produced by γ interactions) passing through a dielectric material with $v > c_0/n$ → **prompt** Cherenkov light

Excellent Cherenkov radiator material: **lead fluoride (PbF_2)**

	BGO	LSO	PbF_2
Density (g/cm³)	7.1	7.4	**7.77**
μ_{511keV} (cm^{-1})	0.96	0.87	**1.06**
Photofraction for 511 keV	0.41	0.32	**0.46**
Raise time (τ_r)	2.8 ns	70 ps	
Decay time (τ_d)	300 ns	40 ns	
Light yield/511 keV (LY)	3,000	15,000	**10** (‡)

(‡) in the 250-800 nm wavelength interval

PbF_2 properties:

- excellent γ stopping properties

- pure Cherenkov radiator (no scintillations)

- excellent optical transmission (down to 250 nm), high refractive index (n ~ 1.8)

- low price (**1/3 BGO, 1/9 LSO**)

Mao, IEEE TNS 57:6 (2010) 3841

TOF-PET with Cherenkov light detection: proof of principle

S. Korpar et al, NIM A654 (2011) 532

Two detectors (back-to-back)
- 25 x 25 x 15 mm^3 crystals (black painted or Teflon wrapped)
- MCP-PMT (Hamamatsu, same as in the Belle II TOP counter)
- ^{22}Na source

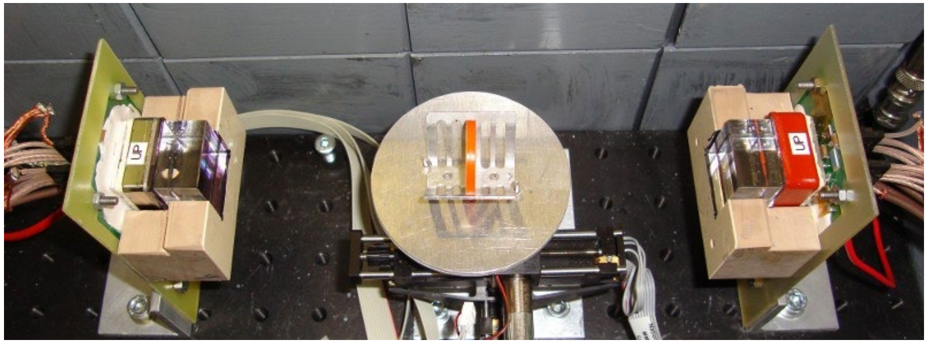

- 15 mm long crystal: FWHM ~ 95 ps
- 5 mm long crystal: FWHM ~ 70 ps

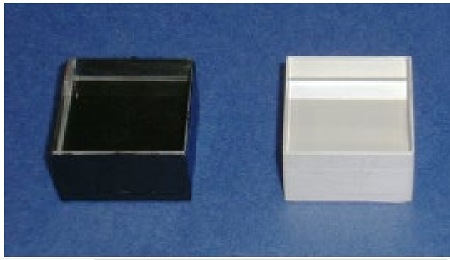

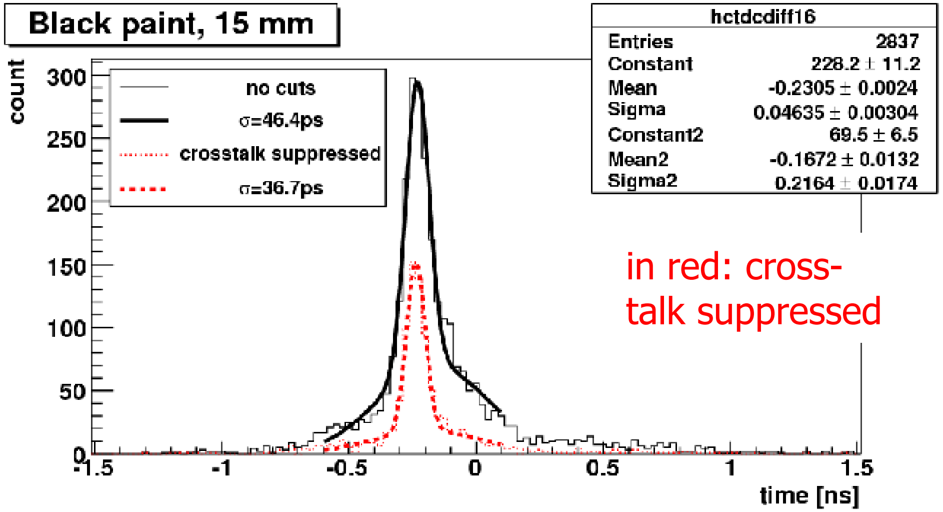

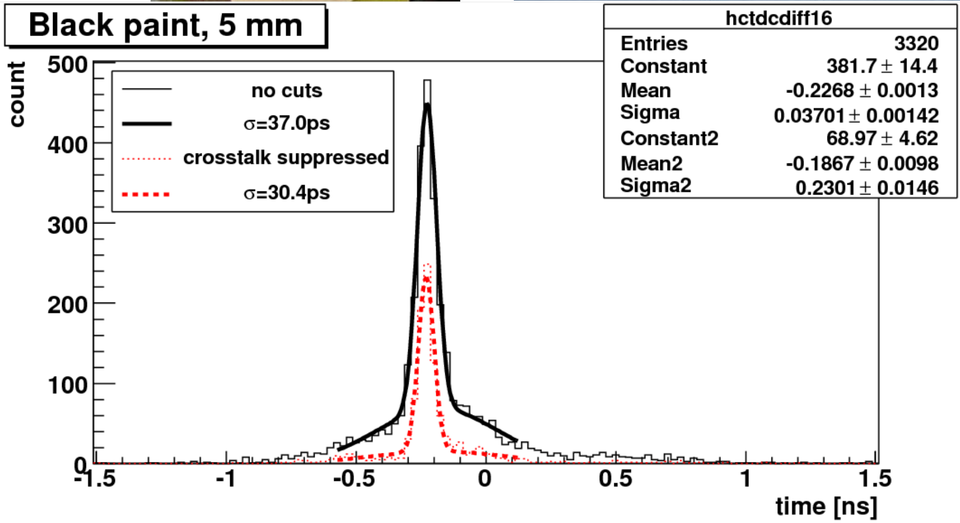

Point source position

Data taken at three ^{22}Na point source positions spaced by 20 mm:

- average time shift 125 ps
- timing resolution ~ 40 ps rms,

  ~ 95 ps FWHM
- position resolution along line of response ~ 6 mm rms,

  ~ 14 mm FWHM

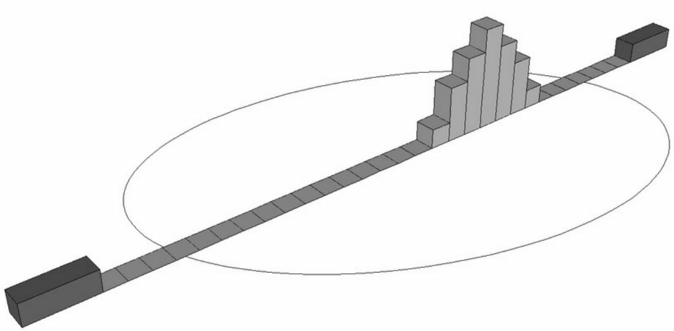

Black painted 15 mm PbF_2 crystals.

S. Korpar et al, NIM A654 (2011) 532–538

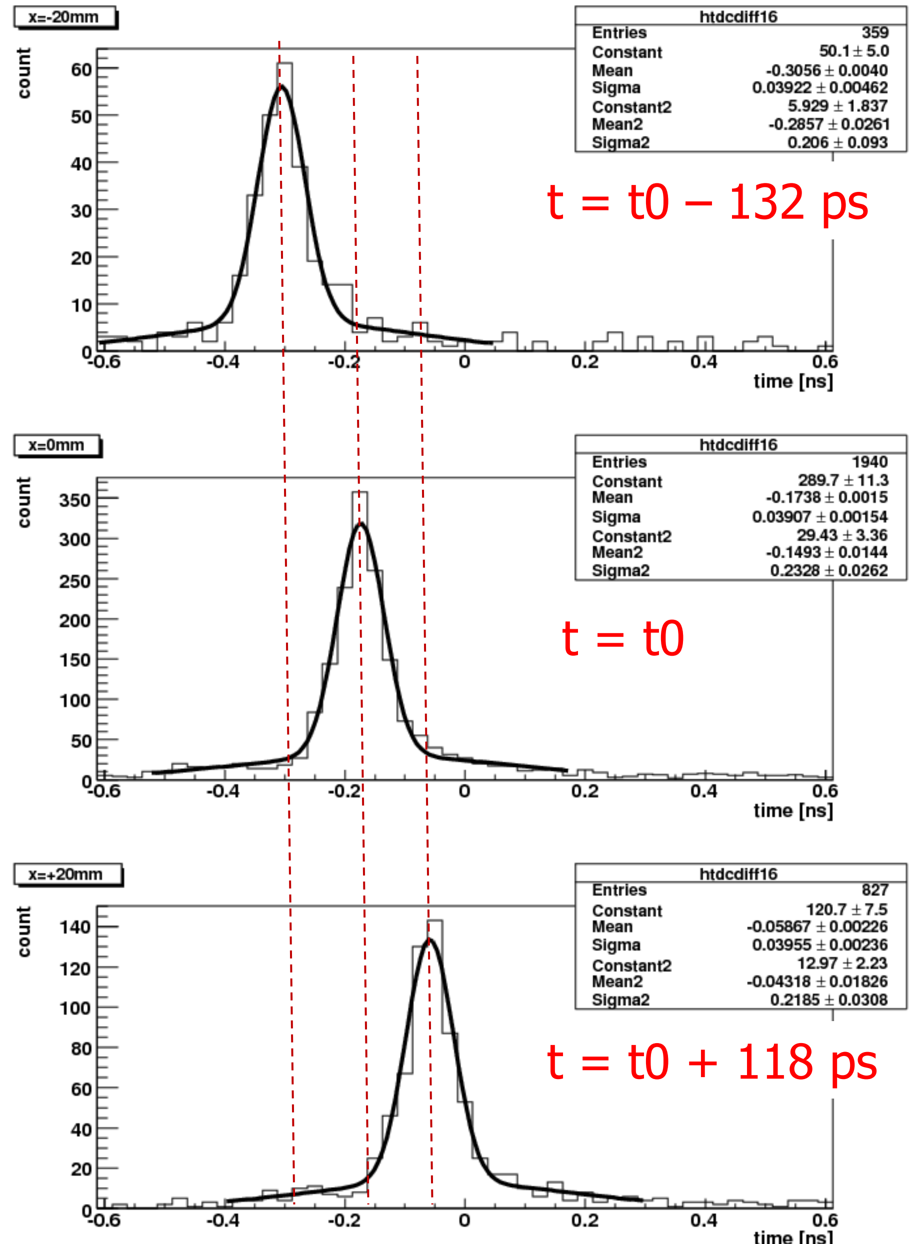

Previous results

(25 * 25 * **15**) mm³ **PbF_2** (black)
+ (22.5 * 22.5) mm² **MCP-PMT**

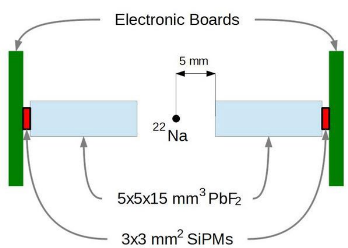

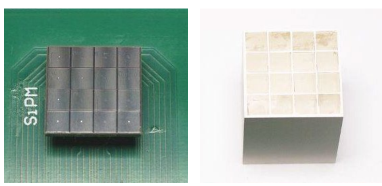

4x4 array:
(3 * 3 * **15**) mm³ **PbF_2** (reflector)
+ (3 * 3) mm² **SiPM**

Multi-layer: 3 x
[(3 * 3 * **5**) mm³ **PbF_2** (black)
+ (3 * 3) mm² **SiPM**]

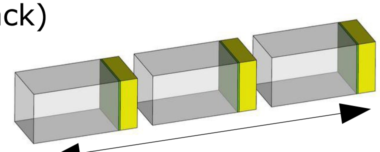

Result	Reference
Cherenkov TOF PET, TOF: **95 ps** FWHM	Korpar, NIM A 654 (2011) 532
With SiPMs, TOF: **306 ps** FWHM	Dolenec, IEEE TNS 63:5 (2016) 2478
Cherenkov PET module: Single side efficiency: **35 %**	Dolenec, NIM A 952 (2020) 162327
Multi-layer detector (simulation) TOF: **22 ps** FWHM before photodetector timing	Consuegra, Phys.Med.Biol. 65(5) (2020) 055013

Limitations of Cherenkov TOF-PET

- Only 10-20 photons created → **only a few detected**
  - efficient photodetector and light collection needed

→ **SiPM**

- **Optical photon travel time spread** in the crystal
  - remaining limitation to TOF resolution

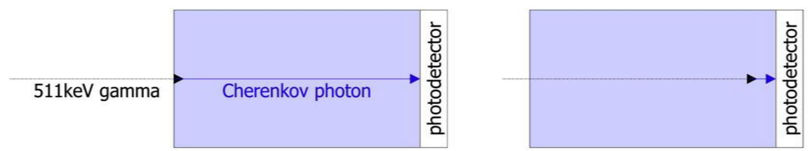

→ **multi-layer**

d = 15 mm, n = 1.8: $t = d \cdot n/c_0 = 90$ ps $t = d/c_0 = 50$ ps → $\Delta t = 40$ ps

- Limited suppression of **scattered events**:
  - only a few Cherenkov photons detected
    → no energy information
  - detection efficiency drops at low gamma energies
    → intrinsic suppression

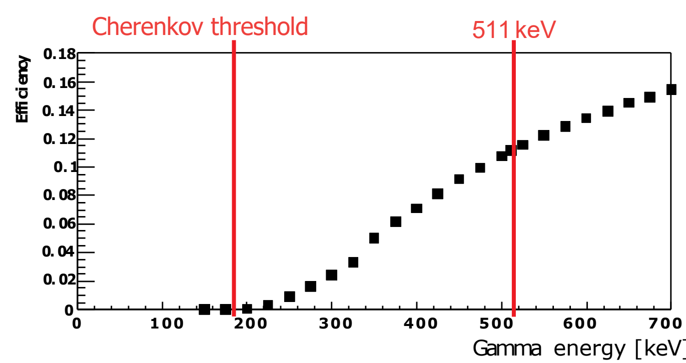

Simulation, PbF_2 with MCP-PMT photodetector

Effect of remaining scatter on image quality?

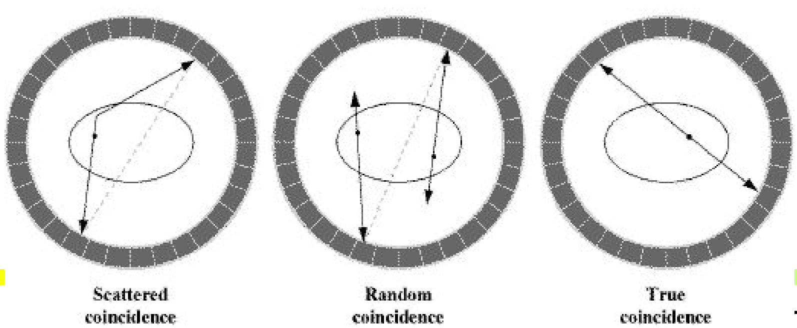

Essential question → MC simulation to evaluate the effect →

Whole-body scanner simulations

Simulation: GATE v8.1

Geometry:

- Based on Siemens Biograph Vision PET/CT
  - ring: 19 modules (Axial FOV: 26.3 cm)
  - module: 2 x 8 block detectors
  - block detector: 4 x 2 mini-blocks
  - mini-block: 5 x 5 crystal array
  - crystal: 3.2 x 3.2 x 20 mm^3

Optical simulations (Cherenkov):

- Surfaces: Geant4 UNIFIED model
  - reflector (diffuse, R=95%, n=1.0)
  - black (R=0%, n=1.5)
- Photodetector: Hamamatsu S14520 SiPM
  - Single Photon Time Resolution (SPTR): 70 ps FWHM
  - SiPM dark counts not modeled

Reconstruction: CASToR v3.1.1

Custom double Gaussian TOF kernel

OSEM-8it:5sub, 1.6 mm voxel, 5 mm filter

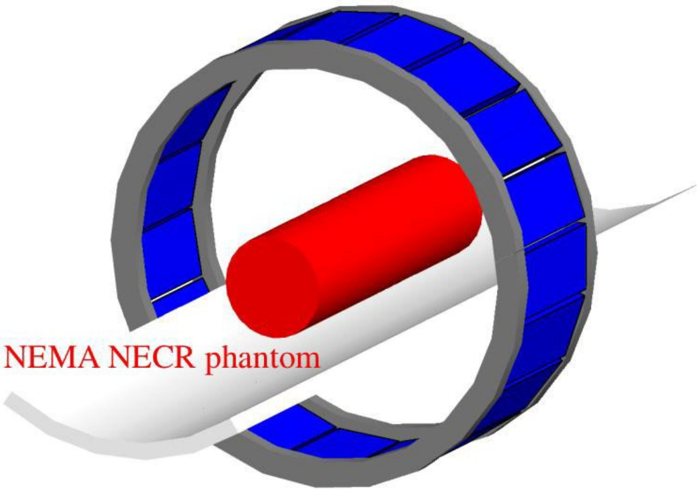

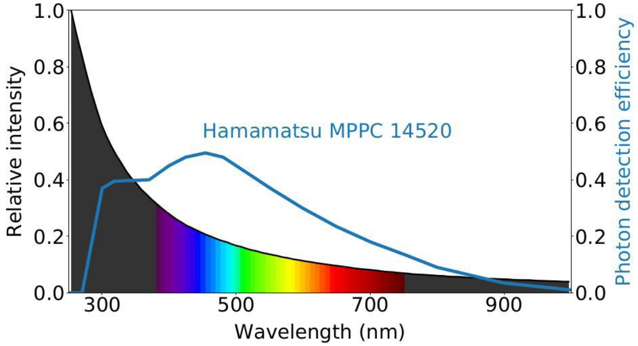

Crystal readout configurations

Reference scanner

- LSO scintillator
- Energy window: 435-585 kev
- Energy resolution: 10%
- CTR: 214 ps

Simulation:

- Cherenkov photon generation, propagation simulated
- Timing defined by first optical photon detected

	Cherenkov detector	Surface treatment	ε^2 (%)	CTR-FWHM (ps)		FOM	
				0 ps SPTR	70 ps SPTR	0 ps SPTR	70 ps SPTR
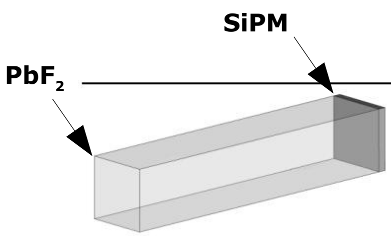	1-sided-back	Black	8.6	100.7	145.5	0.85	0.59
		Reflector	35.3	135.7	184.8	2.60	1.91
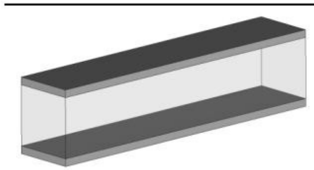	2-sided-top-bottom	Black	26.2	47.0	111.1	5.57	2.36
		Reflector	40.5	48.9	117.8	8.28	3.44
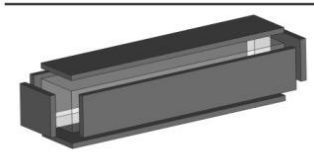	6-sided	/	44.4	54.1	115.4	8.21	3.85

Coincidence detection efficiency: ϵ^2

Figure-of-merit: $FOM = \frac{\epsilon^2}{CTR}$

G. Razdevšek *et al.*, "Exploring the Potential of a Cherenkov TOF PET Scanner: A Simulation Study," IEEE TRPMS 7 (2023) 52, doi: 10.1109/TRPMS.2022.3202138.

SPTR = single photon time resolution

Results: CTR distributions

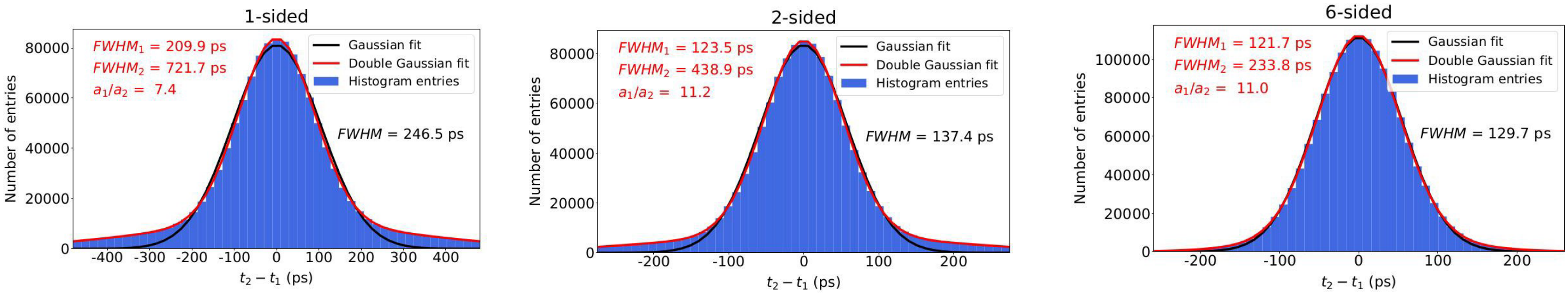

TOF kernel:
-single Gaussian
-double Gaussian

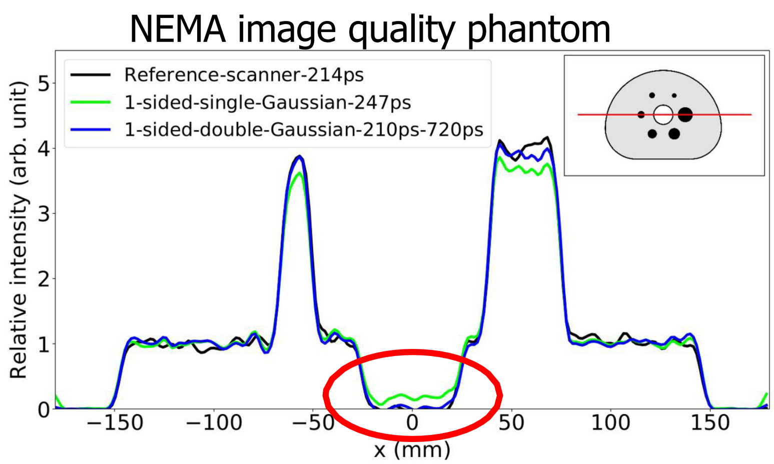

G. Razdevšek *et al.*, IEEE TRPMS 7 (2023) 52

Results: NECR - Noise Equivalent Count Rate

G. Razdevšek *et al.*, IEEE TRPMS 7 (2023) 52

- Noise Equivalent Count Rate*: $NECR = \frac{true^2}{true + random + scatter}$
  - not influenced by TOF
- Scatter Fraction: $SF = \frac{scatter}{true + scatter}$

NEMA NU 2-2018

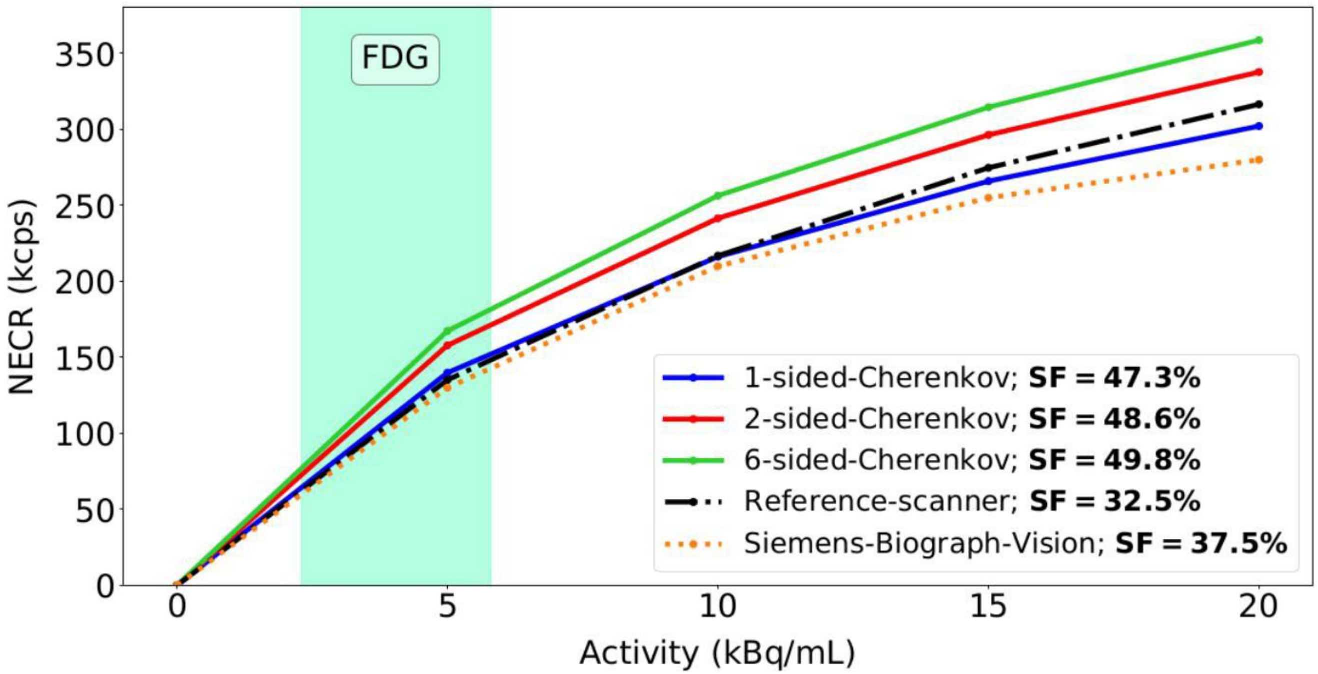

[Sluis, J. Nucl. Med. 60:7 (2019) 1031]

*The “Noise Equivalent Count” is the number of counts from a Poisson distribution (standard deviation estimated by SQRT{N}) that will yield the same noise level as in the data at hand.

Results: Image Quality

NEMA image quality phantom

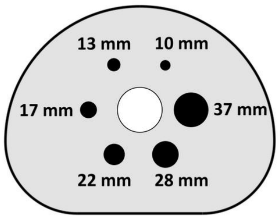

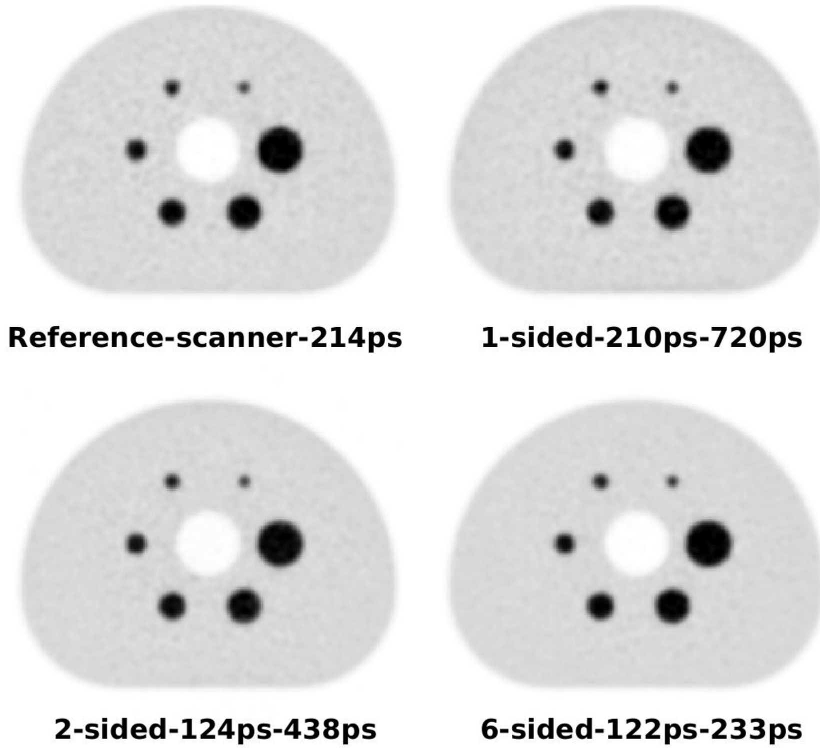

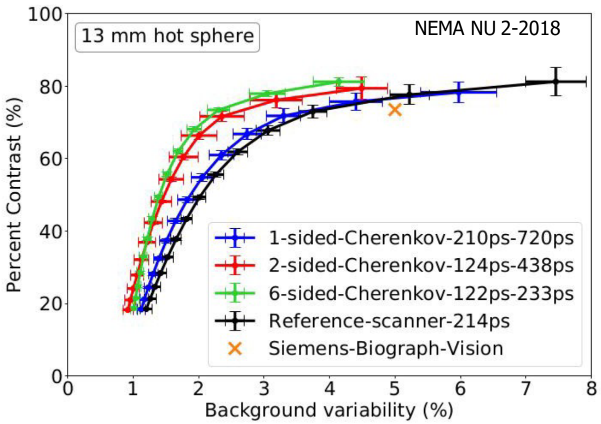

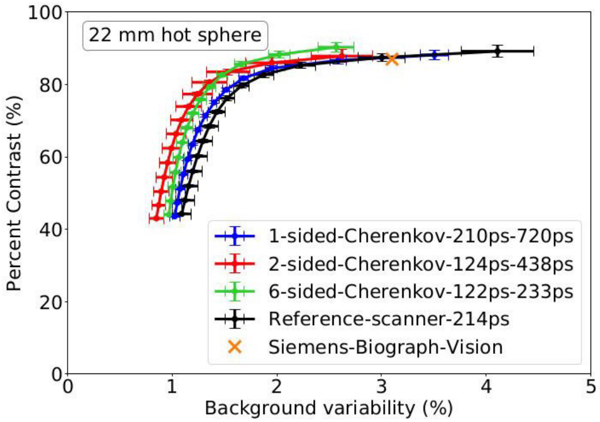

G. Razdevšek *et al.*, IEEE TRPMS 7 (2023) 52

Cherenkov based scanners, conclusion

- Using (exclusively) Cherenkov light in TOF-PET has potential to
  - improve TOF resolution
  - reduce scanner cost (total-body)
- Experiments have demonstrated
  - CTR as low as 30 ps   R. Ota, Phys. Med. Biol. 64 (2019) 07LT01
  - detection efficiency (module) of 35% R. Dolenec et al, NIM A 952 (2020) 162327
- No energy information available → effect on image quality?
- Cherenkov TOF-PET scanner simulations
  - better sensitivity and CTR compensate higher scatter
  - **image quality comparable to state-of-the-art**
- Advanced detector geometries (2-sided top-bottom, multi-layer)
  - even better image quality

G. Razdevšek *et al.*, IEEE TRPMS 7 (2023) 52

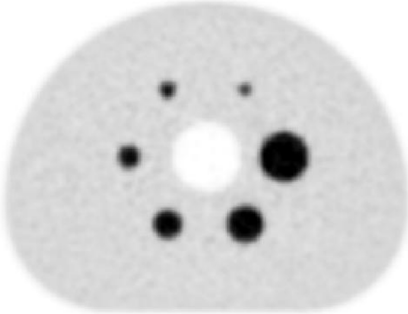

Reference-scanner-214ps

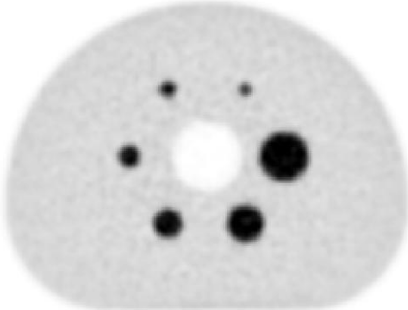

1-sided-210ps-720ps

Cherenkov-based TOF-PET with a large area MCP-PMT

Idea:

- couple short PbF_2 crystals as Cherenkov radiators to the
- LAPPD – a large area MCP-PMT, and make use of the
- flat panel concept

LAPPD with PbF_2 crystals

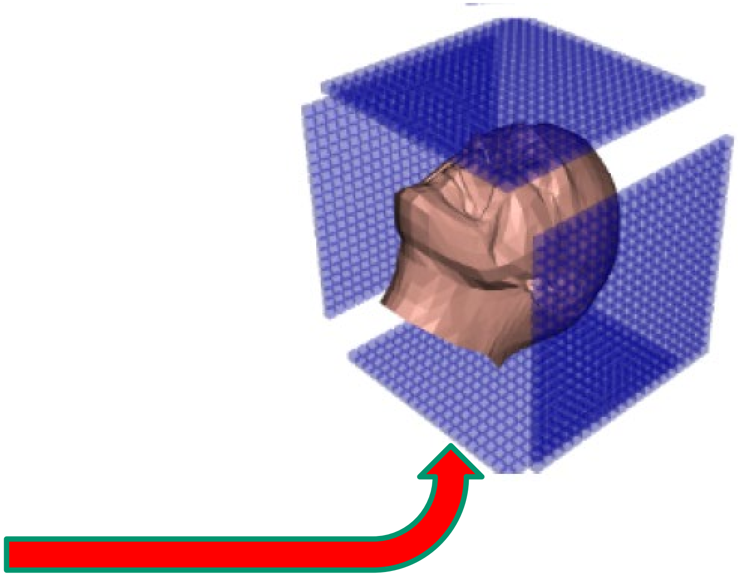

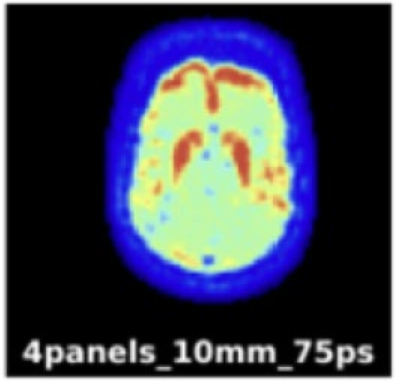

LAPPD with PbF_2 crystals attached to the entry window: an almost ideal flat panel device

CherPET: an ERC (European Research Council) Proof-of-Principle project

LAPPD (large area picosecond photodetector) Gen II

Characteristics (Incom):

- size 230 mm x 220 mm x 22 mm (243 mm x 274 mm x 25.2 mm with mounting case)
- borosilicate back plate with interior resistive ground plane anode – 5 mm thick
- capacitively coupled readout electrode
- MCPs with 20 μm pores at 20 μm pitch
- two parallel spacers (active fraction ≈ 97 %)
- gain $\approx 5 \cdot 10^6$ @ ROP (825 V/MCP, 100 V on photocathode)
- peak QE $\approx 25\%$
- Dark Count rate @ ROP: ~ 70 kHz/cm2 with 8x10^5 gain

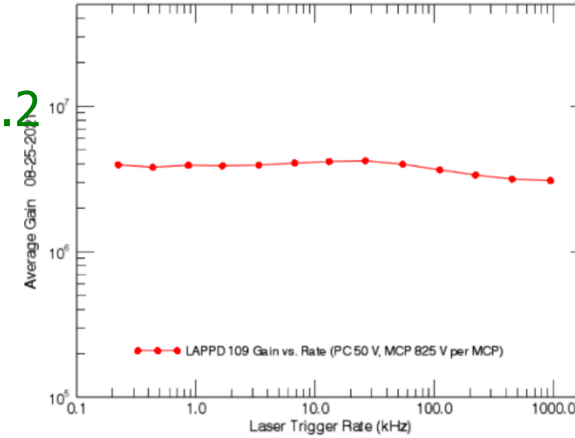

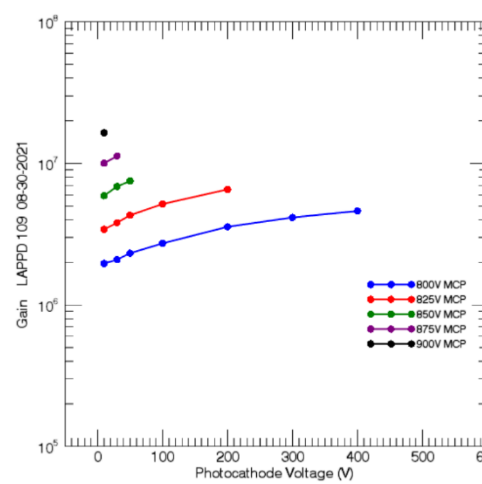

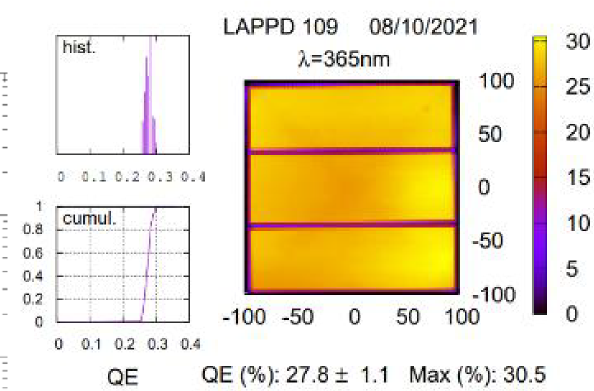

MCP-PMT: single photon pulse height and timing

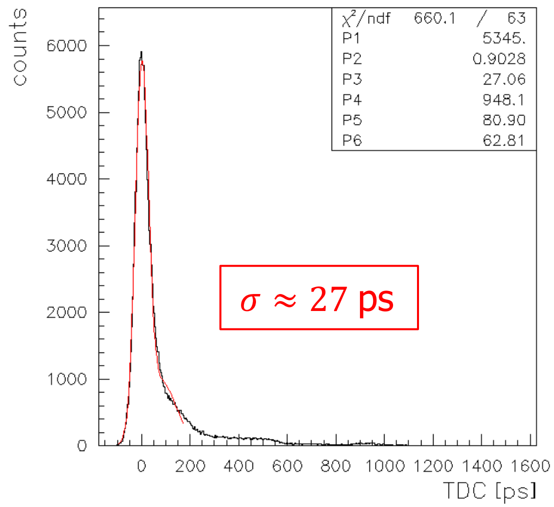

Photoelectron back-scattering produces a rather long tail in timing distribution and position resolution.

Photoelectron backscattering reduces collection efficiency and gain, and contributes to cross-talk in multi-anode PMTs

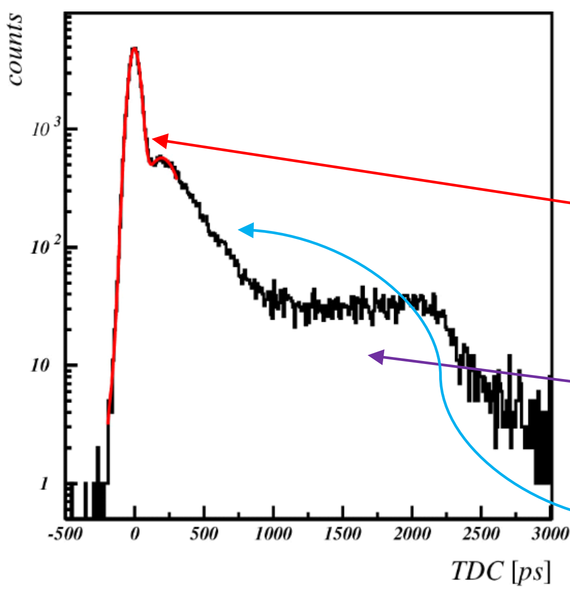

Typical single photon timing distribution with a narrow main peak (σ~30-40 ps) and contributions from photoelectron elastic back-scattering (flat distribution) and inelastic back-scattering.

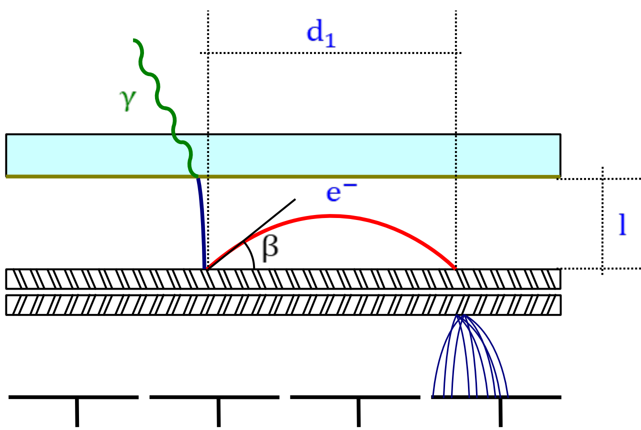

S.Korpar et al, PD07

LAPPD evaluation

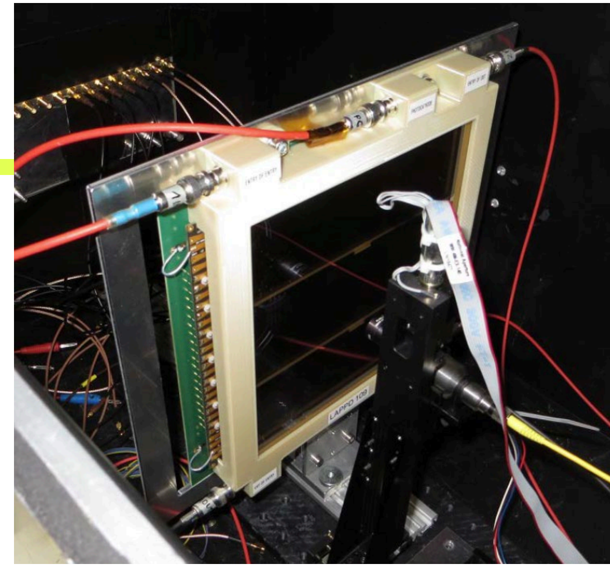

- Two 10 μm devices acquired
- LAPPD installed in the dark box:
- CAEN HiVolta (DT1415ET), 8 Ch Reversible 1 kV/1 mA Desktop HV Power Supply – floating channels
  - 1 kV/1 mA and 0.6 W(!) per channel
- Measure response in the lab with modular electronics, FastIC and PETSys
- Standard setup with QDC, TDC, 3D stage ...
  - TDC value corrected for time-walk
- ALPHALAS PICOPOWER™-LD Series of Picosecond Diode Lasers – 405 nm
  - FWHM ≈20ps
  - light spot diameter on the order of 100μm
- Custom segmentation to study the capacitive coupling and the charge spread

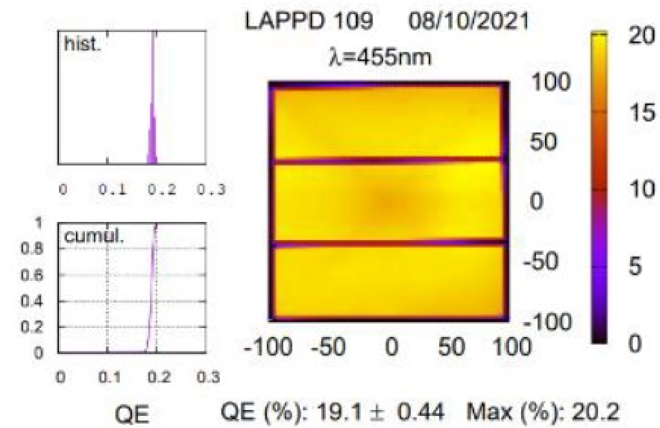

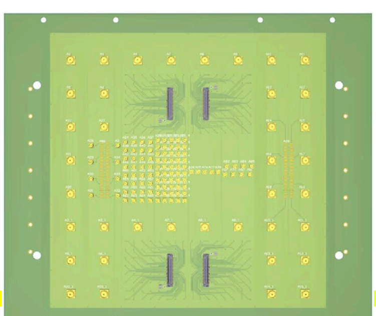

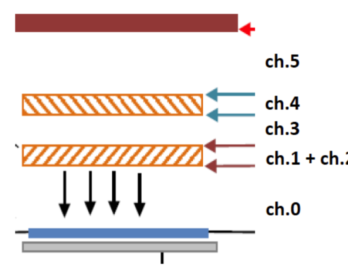

Characterizing MCP-PMT: time resolution and charge sharing

Time difference between downward and sideways initial direction of the photoelectron
(simple model, see backup slides)

$$\Delta t \approx t_0 \sqrt{\frac{E_0}{U e_0}}$$

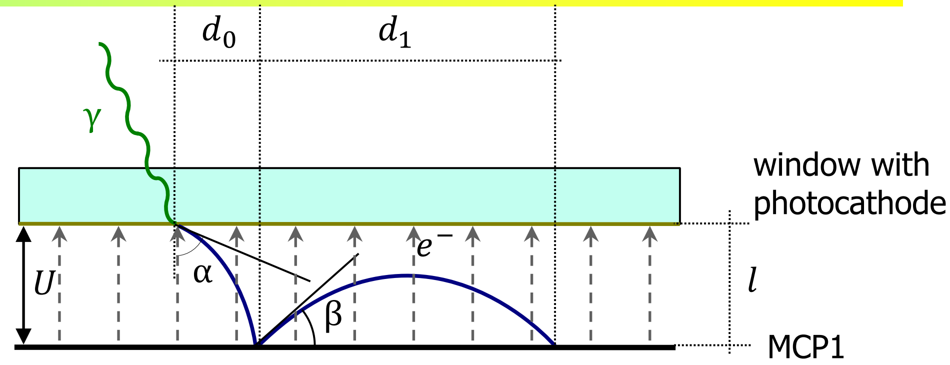

This difference is proportional to the time resolution – sigma of the main peak in the time response of the MCP-PMT

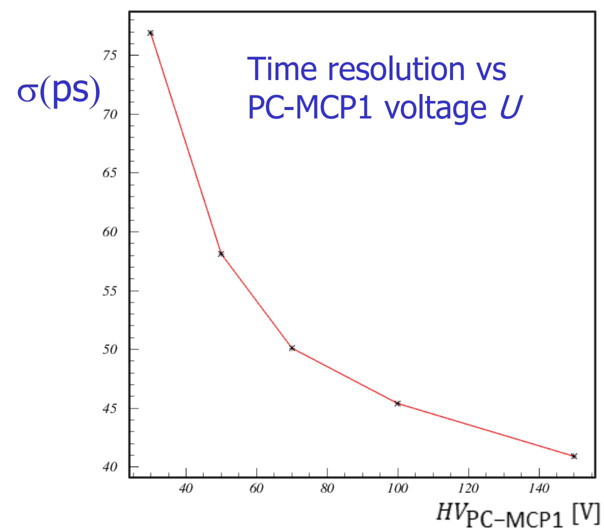

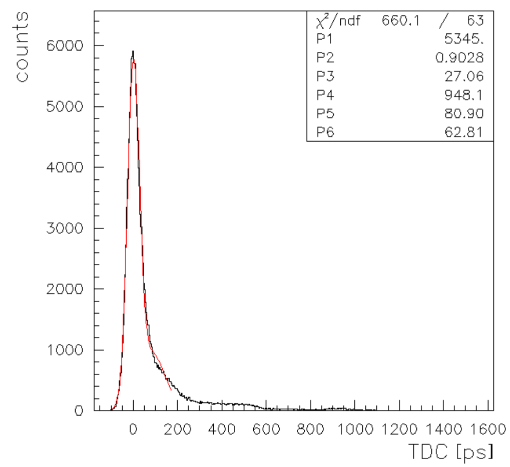

R. Dolenec *et al.*,
NIM A 1069 (2024) 169864

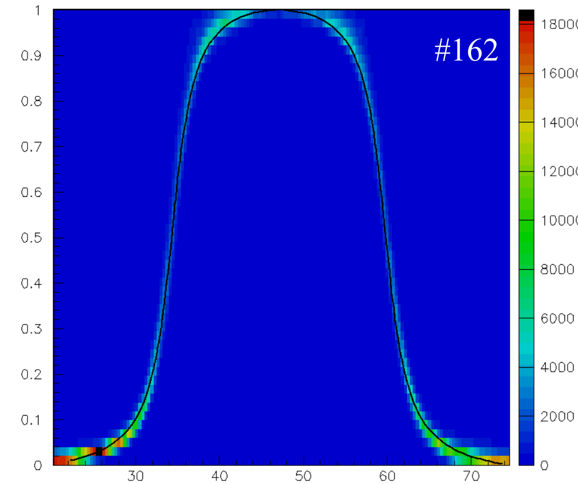

Charge sharing – capacitively coupled read-out electrodes.

Next steps: finalize read-out, attach crystals, test the back-to-back configuration

Summary

The interplay of detector R&D for particle physics and medical imaging has a long history, and this will remain one of the sources of innovation in medical imaging.

Limited angle devices with very fast gamma detection look very promising – lower cost, flexibility in use, affordable total-body scanner.

Cherenkov radiation based annihilation gamma detectors offer a promising method for very fast detection and potentially cheaper devices.

More slides

Micro Channel Plate PMT (MCP-PMT)

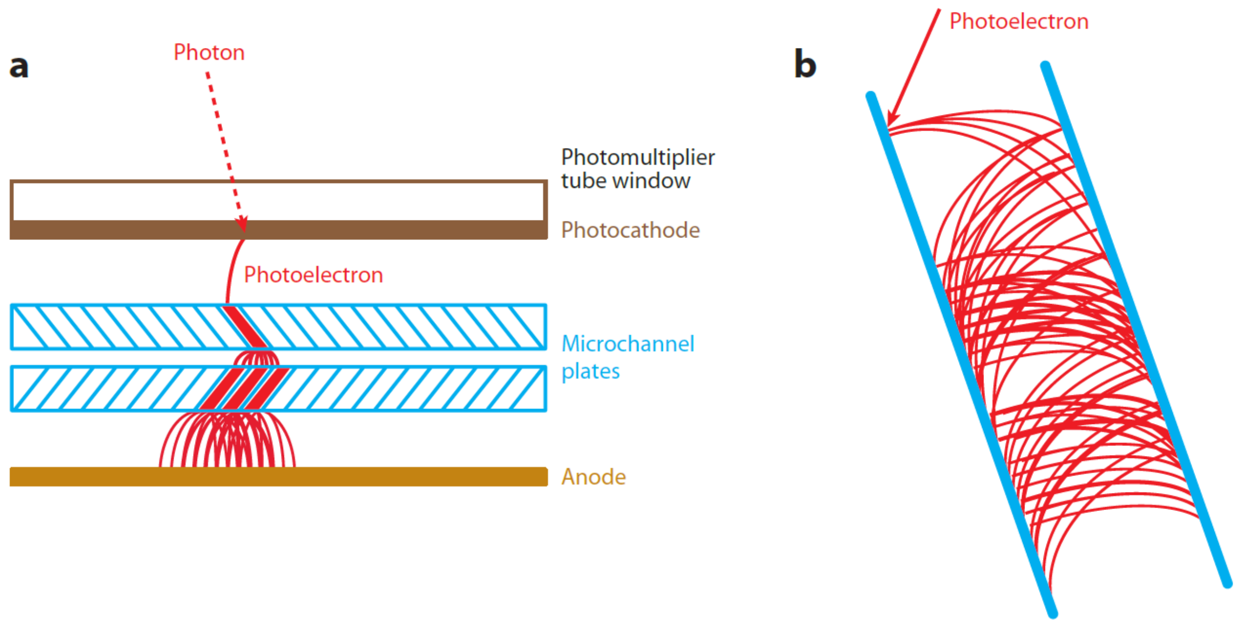

~10-100 μm diameter

Multiplication step: a continuous dynode – a micro-channel coated with a secondary emitter material

Micro Channel Plate PMT (MCP-PMT)

Similar to ordinary PMT – the dynode structure is replaced by MCPs.

Basic characteristics:

- Gain ~ 10^6 → single photon
- Collection efficiency ~ 60%
- Small thickness, high field → small TTS
- Works in magnetic field
- Segmented anode
  → position sensitive

MCP is a thin glass plate with an array of holes (<10-100 μm diameter) - - a continuous dynode structure

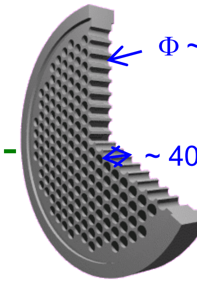

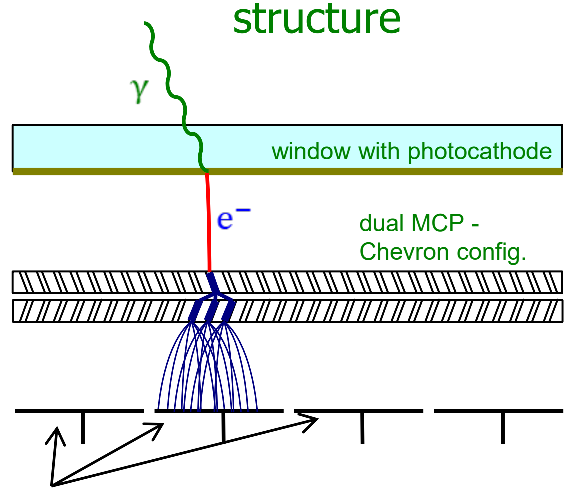

Anodes → can be segmented according to application needs

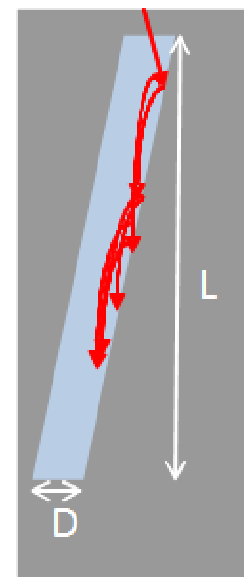

MCP gain depends on L/D ratio – typically 1000 for L/D=40

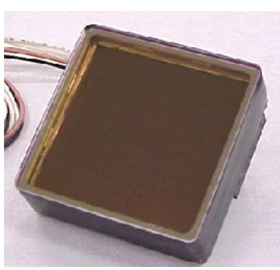

PHOTONIS

HAMAMATSU

1□
□

2□
□ PHOTEK

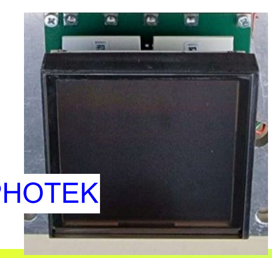

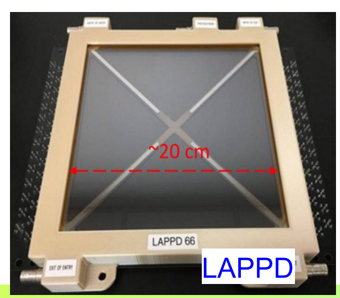

LAPPD

8□
□

Micro Channel Plate PMT: properties

Very fast: single photon detection with sigma of ~30-40 ps

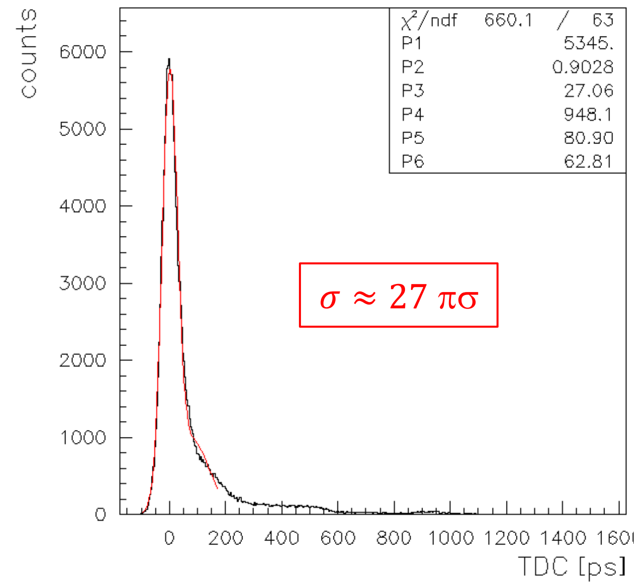

MCP PMTs work well in magnetic fields

→ performance depends on the diameter of the micro-channels

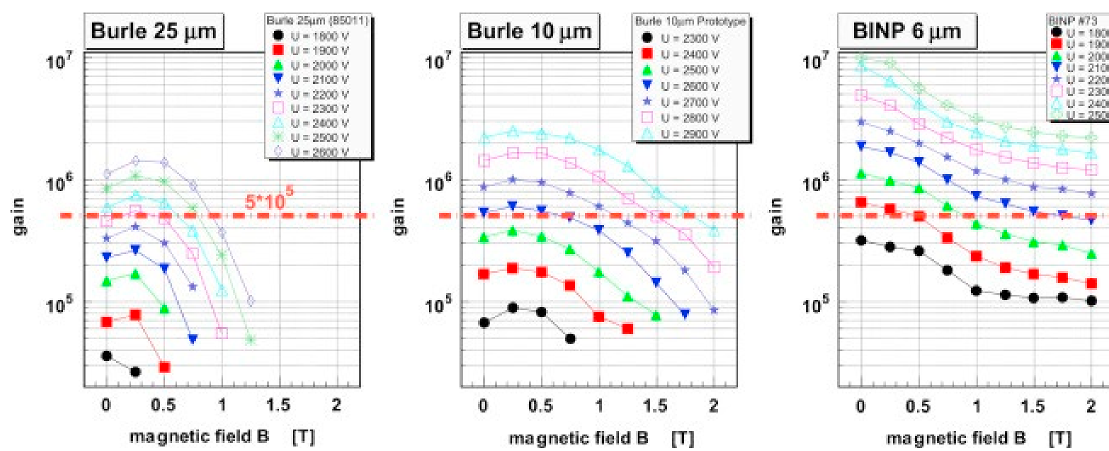

MCP-PMT: single photon pulse height and timing

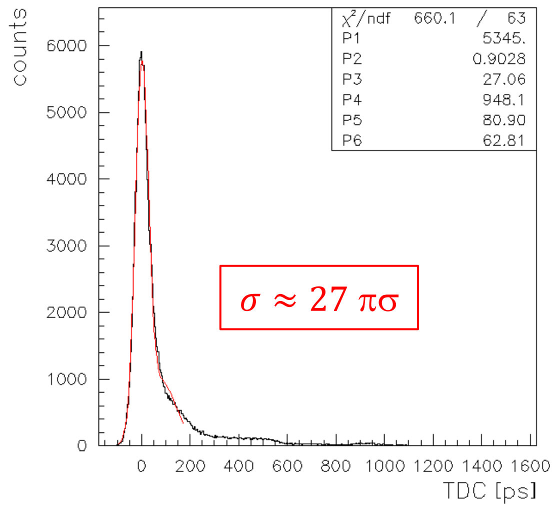

Photoelectron back-scattering produces a rather long tail in timing distribution and position resolution.

Photoelectron backscattering reduces collection efficiency and gain, and contributes to cross-talk in multi-anode PMTs

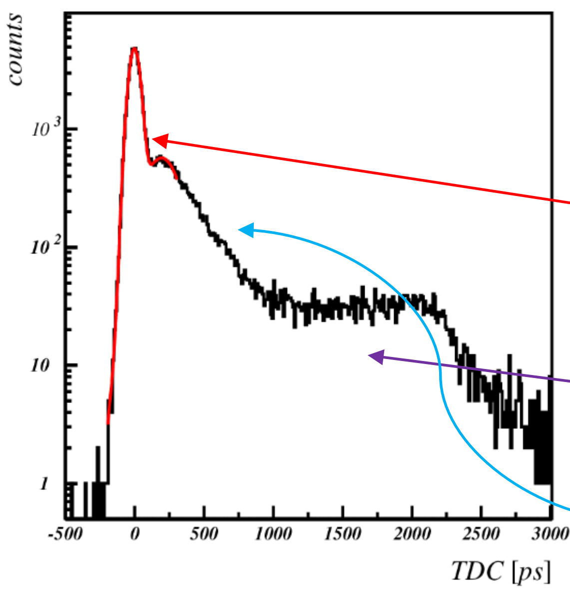

Typical single photon timing distribution with a narrow main peak (σ~30-40 ps) and contributions from photoelectron elastic back-scattering (flat distribution) and inelastic back-scattering.

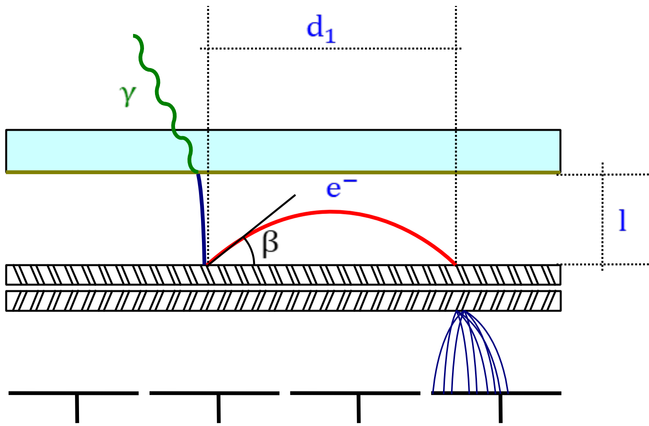

Modelling MCP-PMT: Photoelectrons in a uniform electric field

Photoelectrons travel from the photocathode to the electron multiplier (uniform electric field $\frac{U}{l}$, initial energy $E_0 \ll Ue_0$):

- photoelectron range

$$d_0 \approx 2l\sqrt{\frac{E_0}{Ue_0}}sin(\alpha)$$

- and maximal travel time (sideway start)

$$t_0 \approx l\sqrt{\frac{2m_e}{Ue_0}}$$

- time difference between downward and sideways initial direction

$$\Delta t \approx t_0\sqrt{\frac{E_0}{Ue_0}}$$

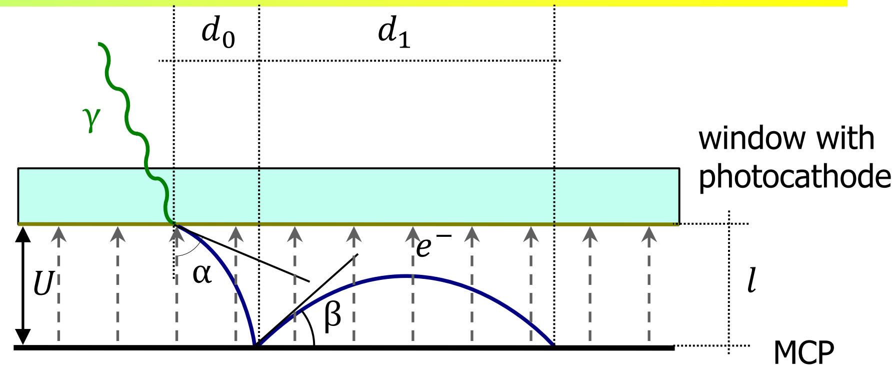

Backscattering delay and range (maximum for elastic scattering):

- maximum range vs. angle

$$d_1 = 2lsin(2\beta)$$

  maximum range for backscattered photoelectron is twice the photocathode – first electrode distance
- maximum delay vs. angle

$$t_1 = 2t_0sin(\beta)$$

  maximum delay is twice the photoelectron travel time
- time of arrival of elestically scattered photoelectrons: flat distribution up to max $t_1 = 2t_0$

Example ($U = 200\text{ V}$, $E_0 = 1\text{eV}$, $l = 6\text{mm}$)

photoelectron:

- max range $d_0 \approx 0.8\text{ mm}$
- p.e. transit time $t_0 \approx 1.4\text{ ns}$
- $\Delta t \approx 100\text{ ps}$

backscattering:

- max range $d_1 = 2l = 12\text{ mm}$
- max delay $t_1 = 2.8\text{ ns}$

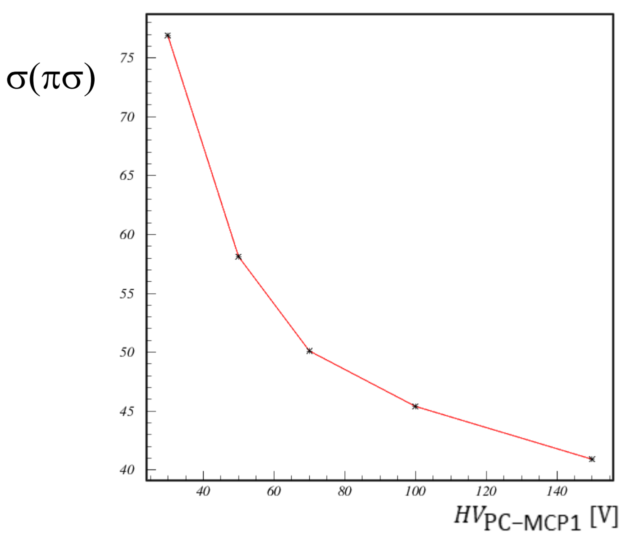

Time resolution vs PC-MCP1 voltage

S.Korpar@PD07

Modular readout system for tests

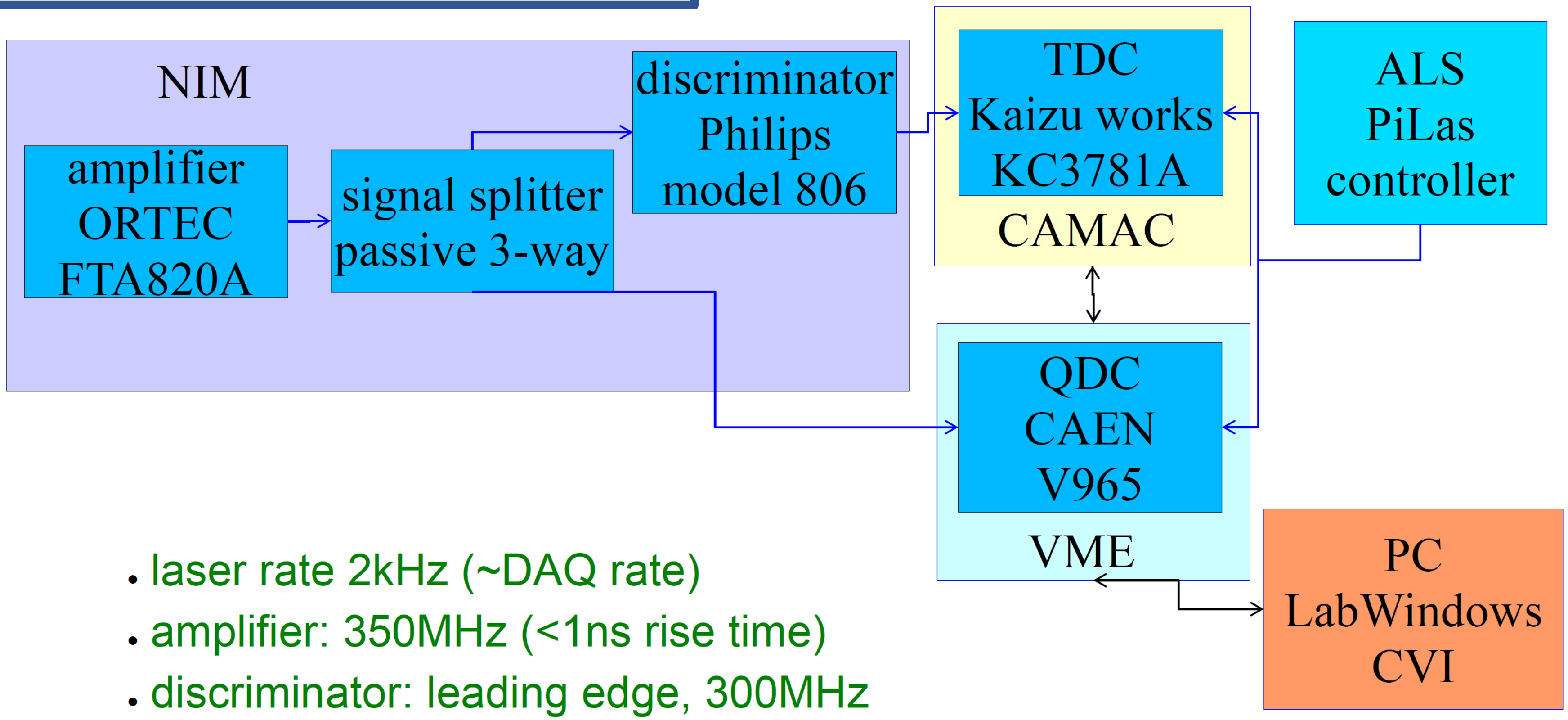

- laser rate 2kHz (~DAQ rate)
- amplifier: 350MHz (<1ns rise time)
- discriminator: leading edge, 300MHz
- TDC: 25ps LSB(σ~11ps)
- QDC: dual range 800pC, 200pC

LAPPD – IJS sensing electrodes

- capacitively coupled electrode produced at IJS with several different patterns:
  - pads: 5 mm, 6 mm, 12.5 mm, 25 mm
  - 50 mm long strips: 5 mm, 3 mm
  - PETSYS connector (256 6mm pads)
  - FastIC connector (12.5 mm and 25 mm pads)

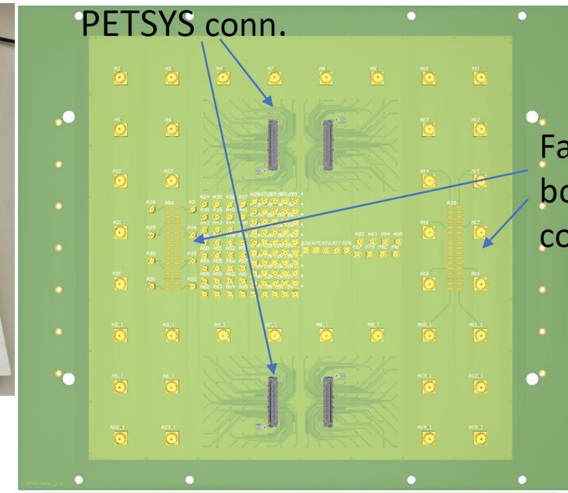

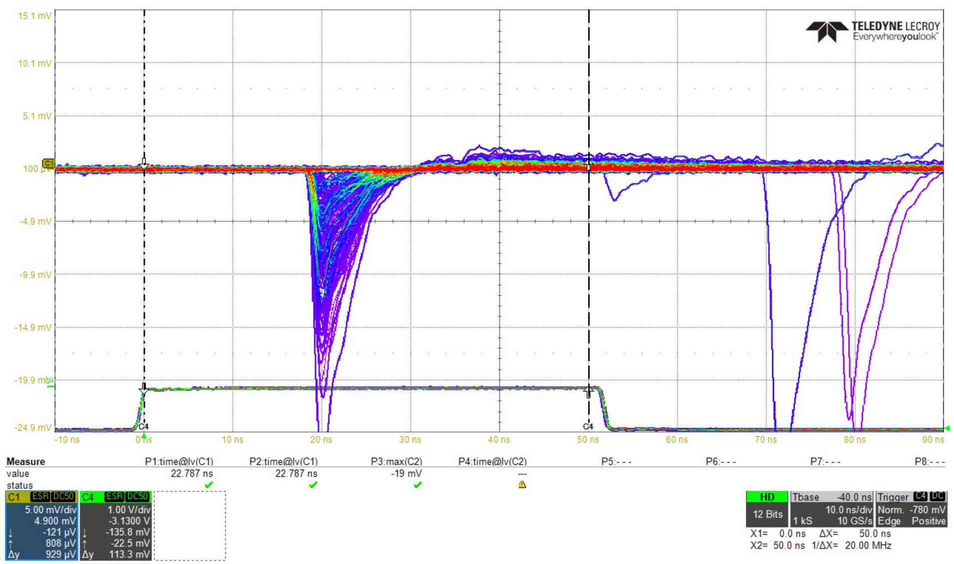

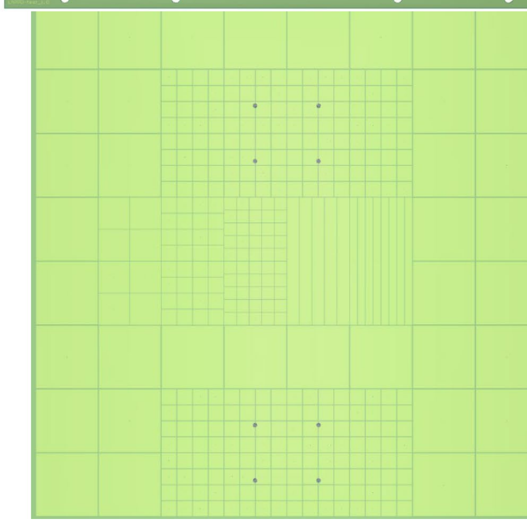

LAPPD – charge sharing in Gen II capacitively coupled electrode readout

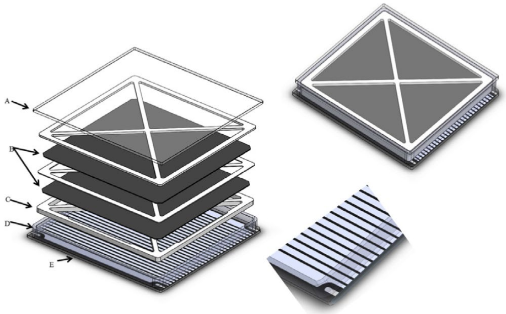

- fraction of the signal on channel 3 vs laser spot x position: $f(x) = \frac{q_3}{\sum_i q_i}$
- scan between the centres of pads 2 and 3 (top)

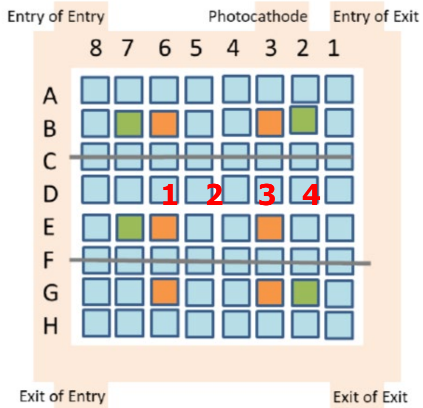

- central slice where signal is equally split between the pads (bottom)
- narrow peak is due to the light spot size and photoelectron spread
- longer tail from photoelectron backscattering - ≈ 6 mm on each side $\rightarrow \approx\ 3$ mm PC – MCP1 distance